Functional Morphology of the Postcranium and Locomotor Behavior of *Neosaimiri fieldsi,* a *Saimiri*-like Middle Miocene Platyrrhine

M. NAKATSUKASA,[1]* M. TAKAI,[2] AND T. SETOGUCHI[3]
[1]*Laboratory of Physical Anthropology, Faculty of Science, Kyoto University, Kyoto 606-01, Japan*
[2]*Primate Research Institute, Kyoto University, Inuyama, Aichi 484, Japan*
[3]*Department of Geology and Mineralogy, Faculty of Science, Kyoto University, Kyoto 606-01, Japan*

KEY WORDS postcranial skeleton; fossil; locomotion; New World monkeys; La Venta, Colombia

ABSTRACT A number of postcranial specimens of *Neosaimiri fieldsi,* a Middle Miocene platyrrhine, were discovered in 1988, 1989, and 1990 at La Venta, Colombia. Until recently only three postcranial specimens of this species had been discovered and the present material adds further information about this taxon's postcranial morphology. In overall skeletal dimensions and in postcranial features, *Neosaimiri* is most similar to *Saimiri* among extant medium-sized platyrrhines, but differs from *Saimiri* in having more rugose surface markings, a longer olecranon, a smaller anterior process of the distal tibia, an absence of a distal surface extension on the anterior tibial shaft, an absence of an anterior midtrochlear depression of the talus, and a shorter distal calcaneus relative to the calcaneal tuberosity. These differences suggest that *Neosaimiri* was relatively heavily built, possessed a more dominant forelimb in quadrupedal progression, and utilized a less stabilized upper ankle joint, and a shorter power arm for plantarflexion. *Neosaimiri* is interpreted as an arboreal quadruped with frequent leaping across arboreal gaps, as in extant *Saimiri,* with perhaps less frequent running and leaping than in *Saimiri.* As with the dentition, the postcranial specimens suggest the close relationship between *Neosaimiri* and extant *Saimiri.* Am J Phys Anthropol 102:515–544, 1997.

During the 1988, 1989 and 1990 field seasons, paleontological expeditions jointly organized by INGEOMINAS (Instituto de Investigaciones en Geociencias, Mineria y Quimica, Colombia) and the Primate Research Institute of Kyoto University discovered numerous fossil primates at the Masato Site in La Venta, west central Colombia (Fig. 1). Among those fossils, dental specimens enabled a revision of the systematics of *Saimiri*-like Middle Miocene platyrrhines: Takai (1994) allocated all of the new dental remains, as well as a mandible that had been attributed to "*Laventiana annectens*" by Rosenberger et al. (1991a), to *Neosaimiri fieldsi*, which had been originally discovered in La Venta in 1949 (Stirton, 1951). As previously advocated by many researchers (e.g., Szalay and Delson, 1979; Rosenberger et al., 1990), the new dental specimens confirm that *Neosaimiri fieldsi* is an ancestral stock of extant *Saimiri* (Takai, 1994).

Contract grant sponsor: Overseas Research Grant from the Ministry of Education, Science and Culture of the Japanese Government; Contract grant number 05041091.

*Correspondence to: Masato Nakatsukasa, Laboratory of Physical Anthropology, Faculty of Science, Kyoto University, Kyoto 606-01, Japan. E-mail nakatsuk@anthro.zool.kyoto-u.ac.jp

Received 23 January 1996; revised 19 November 1996; accepted 6 December 1996.

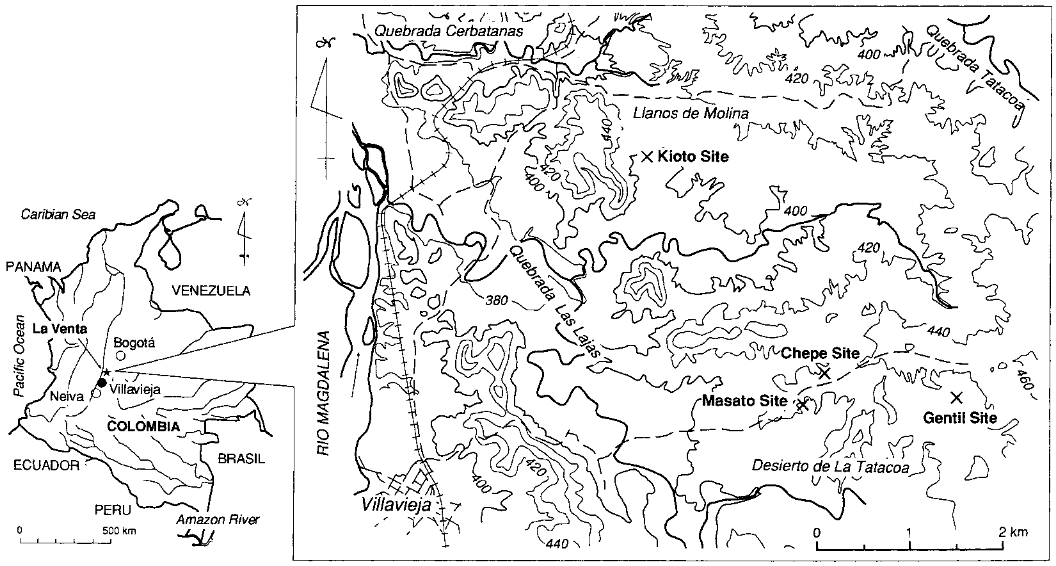

Fig. 1. Map of La Venta (west central Colombia).

In this paper, we report the results of the morphological analysis of 17 postcranial specimens which were collected in association with the dental materials. To date, several postcranial specimens referred to *Neosaimiri* (including "*Laventiana*") have been reported: a talus (Gebo et al., 1990), a distal humerus (Meldrum et al., 1990), and a distal tibia (Meldrum and Kay, 1997). These authors noted that the postcranial morphology of *Neosaimiri* is most similar to that of extant *Saimiri*, and inferred arboreal quadrupedalism and leaping as the most predominant locomotor activities of *Neosaimiri*.

The newly discovered postcranial specimens include a proximal humerus, a proximal ulna, several femoral heads, distal femora, distal tibiae, and a few well-preserved tali and calcanei. This paper adds further information on the postcranium of *Neosaimiri* and discusses its locomotor adaptations by comparisons with extant medium-sized platyrrhines.

MATERIALS AND METHODS

The fossil specimens discussed in this paper are listed in Table 1. All of the specimens were recovered from the Masato Site (=Duke locality 32), about 1.5 × 1.5 m quarry (Fig. 1). The postcranial fossils were collected together with more than 200 isolated teeth by sieving the deposit. Takai (1994; personal communication) attributed these dental remains to 10 or 11 individuals including adult males and females and at least four juveniles. The postcranial remains also include both adult and juvenile materials. However, the juvenile materials are not included in the present study, since they are too fragmentary. Although there are controversies about the taxonomic status of *Saimiri*-like platyrrhines from La Venta (e.g., Rosenberger et al., 1991a), these

TABLE 1. List of fossils

Specimen	Side	Description
IGM-KU		
89171	L	proximal humerus
89174	L	proximal ulna
89181	L	femoral head with partial neck
89182	R	femoral head
89183	L	femoral head
89184	L	femoral head
89185	L	femoral head
89187	L	distal femur
89188	R	distal femur
89189	L	distal femur
89194	L	distal tibia
89195	R	distal tibia
89030	L	partial talus
89031	L	talus
89199	R	talus
89202	L	calcaneus
89203	L	calcaneus

postcranial fossils are tentatively referred to as *Neosaimiri*, adopting the taxonomic opinion of Takai (1994). The assignment of these postcranial specimens to a single taxon will be discussed later.

From La Venta, three postcrania of *Neosaimiri* (including "*Laventiana*") were previously discovered. Among them, a talus (IGM-KU 88003: Gebo et al., 1990) and a distal tibia fragment (IGM 250436: Meldrum and Kay, 1997) were discovered from the same site as the present materials, so these two specimens were treated together with the present materials.

In order to infer the locomotor repertoire of *Neosaimiri*, postcrania of five medium-sized platyrrhine genera (*Saimiri, Aotus, Saguinus, Cebus,* and *Pithecia*) were examined (Table 2). The locomotor modes of these genera are documented in previous studies: *Saimiri sciureus* engages in active above-branch running and frequent leaping (Fleagle and Mittermeier, 1980; Terborgh, 1983). Leaping occupies 42% of the traveling bouts (Fleagle and Mittermeier, 1980) (in the following, the term *Saimiri* is used for *S. sciureus* although another species *S. oerstedii* is known to be a less frequent leaper: see Boinski, 1989). Although the precise locomotor behavior of the nocturnal *Aotus* is not well described quantitatively, this species is described as a predominantly quadrupedal animal, and also an adept but less frequent leaper (Moyniham, 1976; Wright, 1981; Fleagle, 1988). The locomotor modes of *Saguinus* are primarily quadrupedal walking and running, and leaping (Fleagle and Mittermeier, 1980; Garber, 1991). Frequency of leaping varies in *Saguinus* spp.: for example, *S. mystax* leaps at the frequency of 31% during travel (Garber, 1991) and *S. midas* at 24% (Fleagle and Mittermeier, 1980). In the locomotor behavior of *Cebus,* above-branch walking is the predominant locomotor pattern followed by moderately frequent climbing and leaping (Fleagle and Mittermeier, 1980; Gebo, 1993). *Pithecia* engages in leaping most frequently among these platyrrhine genera and is also a frequent quadrupedal walker and climber (Fleagle and Mittermeier, 1980; Fleagle and Meldrum, 1988; Walker, 1994). The frequency of leaping is 47% during traveling (Walker, 1994). This species characteristically shows clinging postures on tree trunks and lianas (Fleagle and Meldrum, 1988; Walker, 1994).

TABLE 2. List of comparative specimens

Genus	Species	Male	Female	Unknown	Total
Saimiri	*sciureus*	12	11	2	25
Aotus	*lemurinus*	1	4	1	6
	azarae	6 (4)[1]	1	0	7 (5)
	trivirgatus	2	4 (3)	0	6 (5)
	Total				19 (16)
Saguinus	*midas*	2 (4)	1	4 (3)	7 (5)
	mystax	5 (4)	2	2 (1)	9 (7)
	Total				16 (12)
Cebus	*albifrons*	18 (11)	9 (5)	0	27 (16)
Pithecia	*monachus*	6	1 (0)	0	7 (6)
	pithecia	3 (2)	0	0	3 (2)
	Total				10 (8)

[1] Parentheses indicate number of talar specimens if different.

The extant comparative specimens are housed in the Field Museum of Natural History (Chicago, IL), the American Museum of Natural History (New York, NY), and the Primate Research Institute, Kyoto University (Inuyama, Japan). Thirty dimensions of postcranial specimens were measured. Definitions of the measurements are schematically shown in Figure 2. Each measurement was obtained to the nearest tenth of a mm by using a digital sliding caliper. Measurements were taken in the right side if available. Statistical differences were tested for by multiple comparison Fisher's Protected Least Signifciant Difference (PLSD) at a significance level of 5%. Statistical calculations were performed using StatView (Abacus Concepts, Inc., Berkeley, CA).

RESULTS

Humeral head (Fig. 3)

Description. IGM-KU89171 is a left proximal humerus. Its proximodistal length is about 12 mm. The articular surface of the head is elongated superoinferiorly, with the transverse diameter being 85% of the sagittal diameter. In superior view, the medial and lateral borders of the articular surface make a modestly wide angle (about 70°). Although the superior surface is almost symmetrical, the bisector of the articular surface passes through the lateral side of the bicipital groove. The superior surface of the head is evenly convex both mediolaterally and anteroposteriorly. The lateral border of the head is higher than the medial border. Along the lateral border of the head,

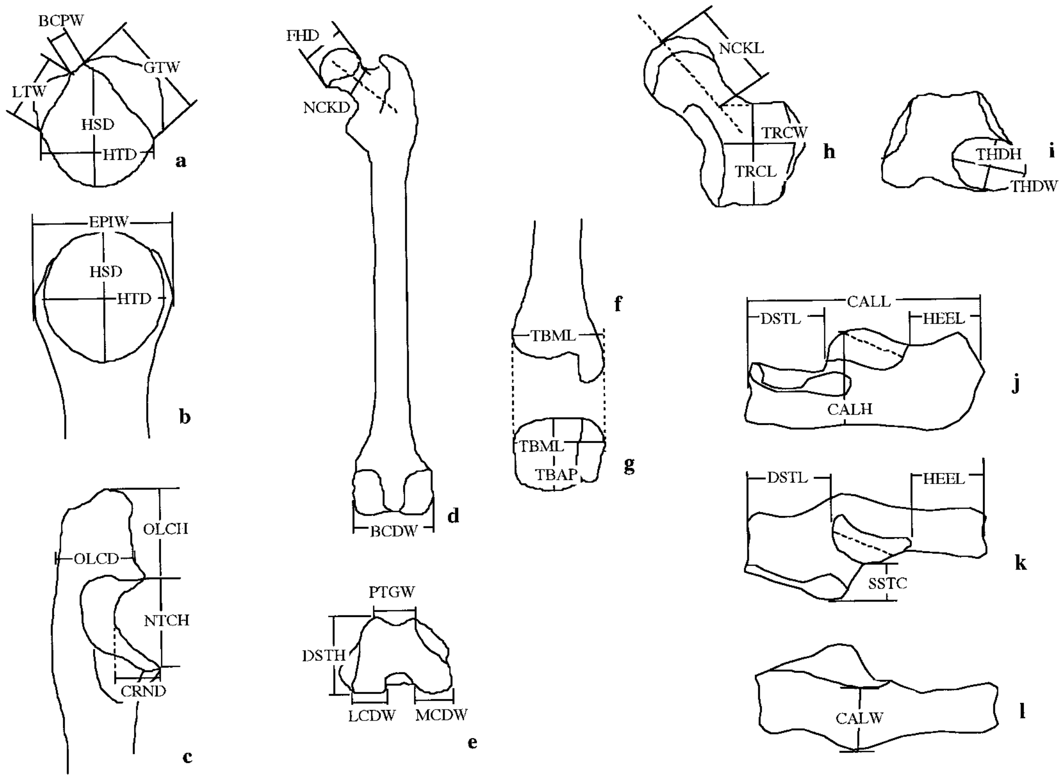

Fig. 2. Schematic explanation of the measurements. **a:** Proximal view of the right humerus. **b:** Posterior view of the right proximal humerus. **c:** Lateral view of the right proximal ulna. **d:** Posterior view of the right femur. **e:** Distal view of the right femur. **f:** Anterior view of the right distal tibia. **g:** Distal view of the right tibia. **h:** Superior view of the right talus. **i:** Distal view of the right talus. **j:** Medial view of the right calcaneus. **k:** Superior view of the right calcaneus. **l:** Plantar view of the right calcaneus. For abbreviations see Tables 3–9.

there is a groove adjacently to the greater tuberosity (Fig. 3a).

The greater tuberosity is lower than the humeral head. Its superior surface is flat and bears a marked insertion of *m. supraspinatus.* The fovea for *m. infraspinatus* is situated on the lateral side of the greater tuberosity. The fovea is large, rounded, and faces laterally. The lesser tuberosity is positioned lower than the greater tuberosity but projects markedly laterally. The surface marking of *m. subscapularis* is very rugose. The bicipital groove is wide and shallow, and positioned slightly anteromedially. The lateral wall of the bicipital groove is low and sharp. The medial wall is obtuse and becomes indistinct inferior to the lesser tuberosity.

The cross-section of the proximal shaft is a trapezoid shape, which is anteroposteriorly slightly compressed. The posterior angle, which buttresses the humeral head, is low and round. The medial and lateral angles, which mark the extent of the insertion of *m. triceps brachii,* are relatively acute. The anterior angle (deltopectoral crest) is also relatively sharp.

Comparison. The overall size of IGM-KU 89171 is similar to that of extant *Saimiri* (Table 3, HTD, HSD, EPIW). The articular surface is as superoinferiorly long as in *Saimiri, Saguinus,* and *Cebus* (Fig. 4, Table 3, HTD/HSD). *Aotus* and *Pithecia* have a more round humeral head. While the humeral head is well expanded beyond the greater tuberosity in all these extant platyrrhines, the groove along the lateral border of the articular surface is present only in *Aotus, Cebus,* and *Pithecia.*

The diameter of the greater tuberosity (GTW/HTD) of the fossil is moderately large

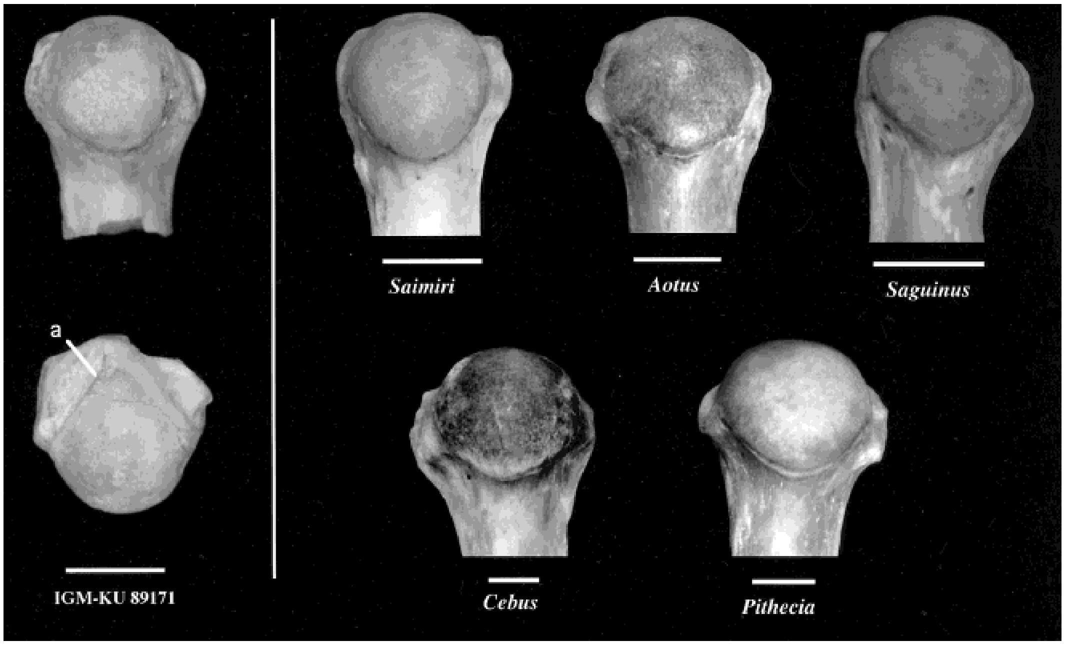

Fig. 3. Right proximal humeri of *Neosaimiri* (IGM-KU 89171) and extant platyrrhines in posterior view. For *Neosaimiri*, the proximal view is also shown. a = a groove adjacent to the greater tuberosity. Scales are changed to an approximately same size. Scale bars = 5 mm.

TABLE 3. Metric variables of the humerus

		HTD	HSD	EPIW	GTW	LTW	BCPW	HTD/ HSD (%)	GTW/ HTD (%)	LTW/ HTD (%)	BCPW/ EPIW[1] (%)
IGM-KU 89171		7.5	8.8	8.9	7.0	4.8	2.7	85.2	93.3	64.0	30.3
Saimiri	Mean	7.32	8.52	9.49	6.87	4.63	2.59	86.43	93.98	63.79	27.26
(n = 25)	S.D.	0.42	0.46	0.62	0.49	0.44	0.30	3.97	4.22	5.57	2.60
	Range	6.4–8.0	7.6–9.4	8.3–10.6	5.9–7.9	3.9–5.6	2.0–3.0	80.5–95.1	87.2–101.3	56.3–73.5	21.7–32.6
Aotus		8.28	9.38	10.39	8.06	4.98	2.87	89.17	96.58	58.56	27.58
(n = 19)		0.57	0.57	0.60	0.56	0.45	0.39	4.26	3.84	4.43	2.65
		7.2–9.2	8.4–10.2	9.5–11.7	7.1–9.0	4.3–6.2	2.2–3.5	80.0–95.2	90.2–102.3	51.7–68.0	21.8–31.8
Saguinus		5.82	6.70	7.57	5.65	3.79	2.23	86.45	95.92	64.00	27.96
(n = 16)		0.54	0.66	0.73	0.63	0.54	0.58	3.39	5.06	4.68	3.82
		5.1–6.6	5.9–7.9	6.6–8.9	4.7–6.9	2.9–5.2	1.6–3.8	81.9–91.7	85.5–102.0	56.9–73.1	22.0–35.4
Cebus		11.94	13.70	15.60	11.62	6.98	4.22	87.10	98.40	60.00	26.77
(n = 27)		1.09	0.87	1.15	0.98	0.76	0.55	2.49	4.56	5.72	2.71
		10.2–14.4	12.1–15.2	13.3–17.4	9.7–13.5	5.6–8.6	3.3–5.4	81.6–92.6	91.9–106.1	51.2–69.9	22.3–32.5
Pithecia		11.25	12.62	13.58	10.31	7.42	3.88	89.40	93.27	66.26	28.45
(n = 10)		0.62	1.02	1.22	1.00	0.60	0.81	4.71	5.02	6.42	3.69
		10.4–12.2	11.1–13.6	11.8–15.3	8.6–11.7	6.4–8.5	2.9–5.1	82.6–95.0	86.9–100.9	56.6–78.0	23.7–34.5

[1] Abbreviations: HTD, transverse diameter of the humeral head; HSD, sagittal diameter of the humeral head; EPIW, proximal epiphysis width; GTW, diameter of the greater tuberosity; LTW, diameter of the lesser tuberosity; BCPW, width of the bicipital groove (see Fig. 2).

as in extant platyrrhines excluding *Cebus* in which the greater tuberosity is more enlarged. The diameter of the lesser tuberosity (LTW/HTD) is similar to that of *Saimiri*, *Saguinus*, and *Pithecia*, but larger than those of *Aotus* and *Cebus*. The bicipital groove width (PCPW/EPIW) of the fossil overlaps with those of extant platyrrhines. The groove is relatively shallow like extant genera except *Cebus* whose groove is more deeply excavated.

Proximal ulna (Fig. 5)

Description. IGM-KU 89174 is a left proximal ulna, broken 3 mm distal to the

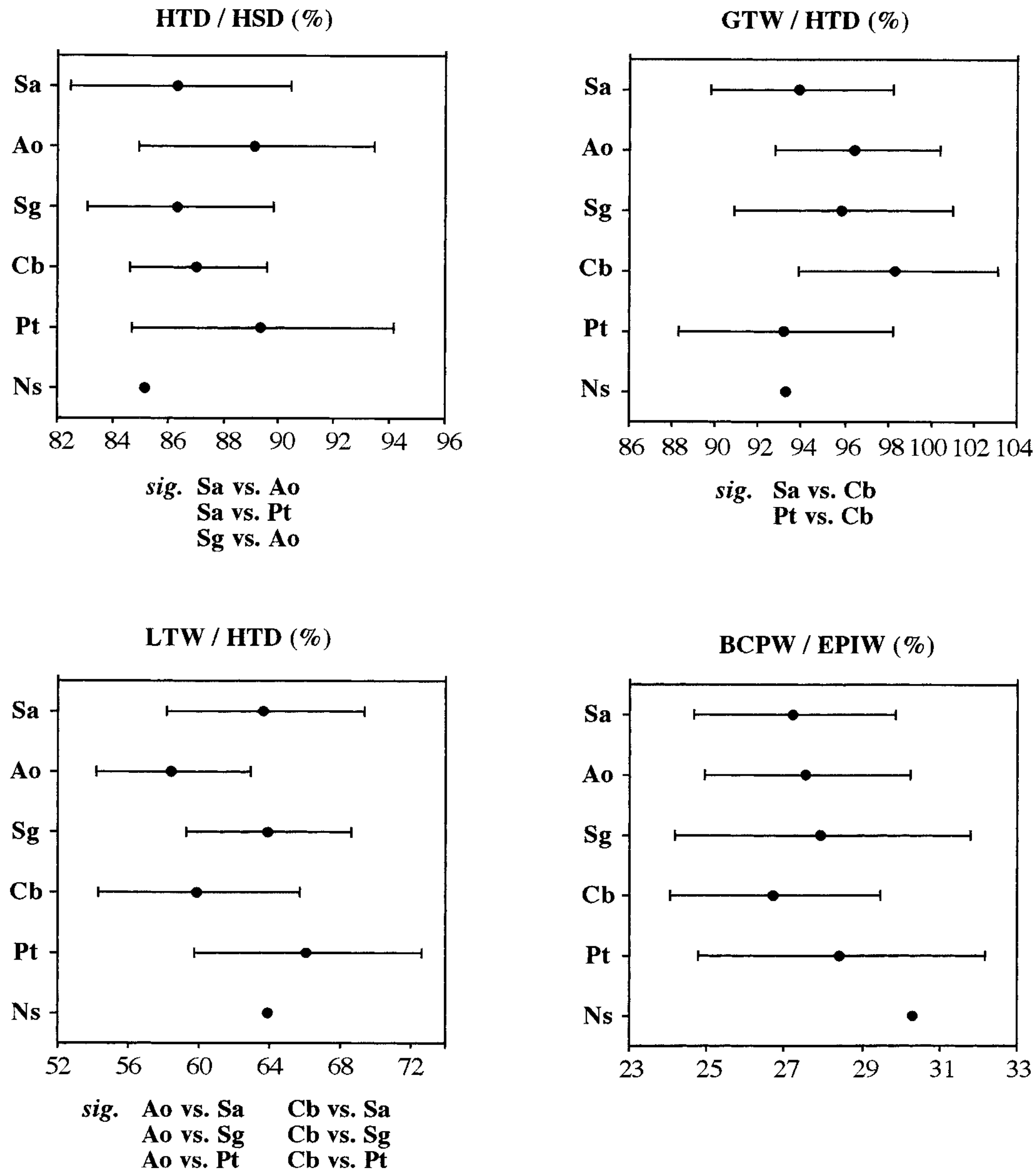

Fig. 4. Mean and ±1 standard deviation of humeral variables. Statistical difference was tested for by multiple comparison (Fisher's PLSD) at $P = 0.05$ and significantly different pairs are shown below each plot. Abbreviations: Sa, *Saimiri;* Ao, *Aotus;* Sg, *Saguinus;* Cb, *Cebus;* Pt, *Pithecia;* Ns, *Neosaimiri.*

radial notch. The superoinferior length is about 16 mm. The olecranon is proximodistally long, straight, and anteroposteriorly thin. The olecranon height is 109% of the trochlear notch height (Table 4, OLCH/NTCH) and the anteroposterior dimension is 81% of the olecranon height (OLCD/OLCH). The superior surface of the olecranon bears a rugosity for *m. triceps brachii* anteriorly. On its medial aspect, the olecranon is very concave in the region of *m. flexor digitorum profundus* (Fig. 5a).

The olecranon beak projects moderately anteriorly. The articular surface of the troch-

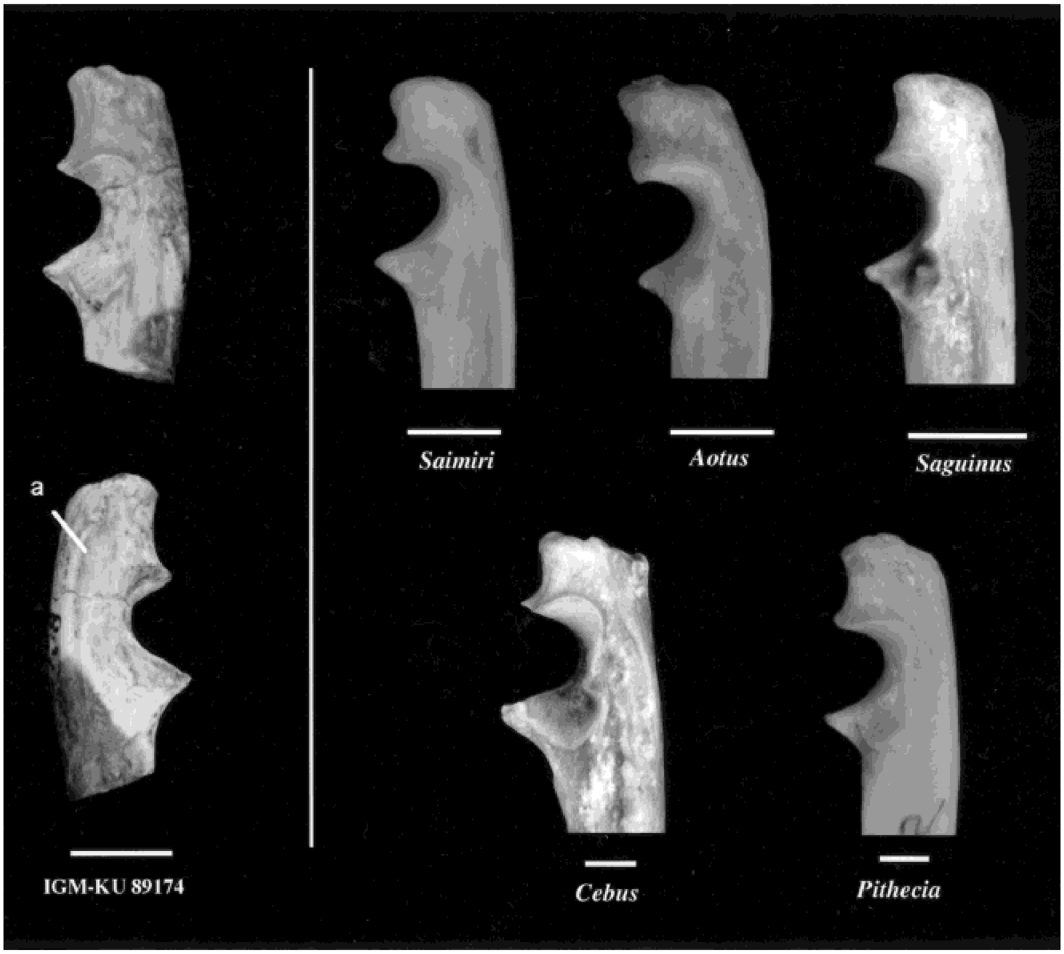

Fig. 5. Left proximal ulnae of *Neosaimiri* (IGM-KU 89174) and extant platyrrhines in lateral view. For *Neosaimiri*, the medial view is also shown (lower). a = a concave. Scales are changed to an approximately same size. The photograph of *Pithecia* is reversed to the left for comparative purposes. Scale bars = 5 mm.

lear notch is raised proximally on the medial and lateral surfaces adjacent to the olecranon beak. The proximolateral extension is slightly exaggerated, giving the articular surface as a whole a modestly twisted shape. The coronoid process projects anteriorly further than the olecranon beak. The coronoid projection is about 64% of the trochlear notch height (CRND/NTCH). The medial border of the coronoid process is somewhat eroded. The coronoid surface is continuous with the radial notch, which is shallow, directed laterally, and tilted slightly.

The shaft is moderately compressed mediolaterally. The mediolateral diameter is about 58% of the anteroposterior diameter at the broken end of the specimen. The insertion of *m. brachialis* lies centrally on the medial surface, slightly proximal to the broken end.

Comparison. The overall size of IGM-KU 89174 is similar to those of *Saimiri* or *Aotus* (Table 4, OLCH, NTCH, CRND). The olecranon of the fossil is disproportionally long as compared with extant platyrrhines. The relative olecranon height (OLCH/NTCH) is beyond the ranges of *Saimiri*, *Aotus* and *Pithecia*, and close to the average of *Saguinus*, which has a especially long olecranon (Fig. 6, Table 4). The anteroposterior diameter of olecranon (OLCD/OLCH) of the fossil is below the ranges of the extant genera. Al-

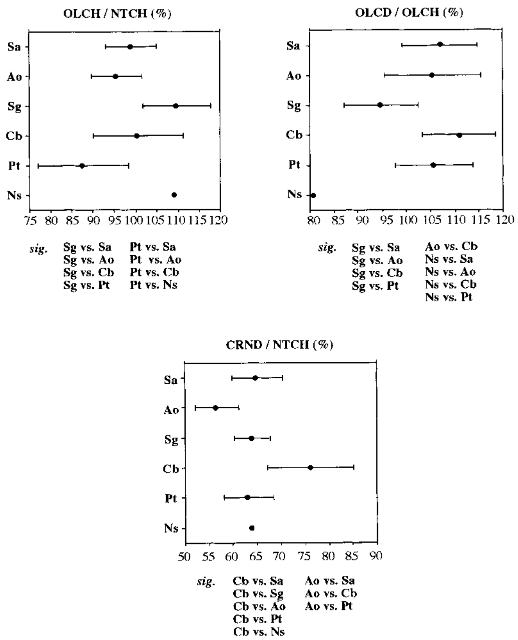

Fig. 6. Mean and ±1 standard deviation of ulnar variables. Statistical difference was tested for by multiple comparison (Fisher's PLSD) at $P = 0.05$ and significantly different pairs are shown below each plot. For species name, see Figure 4.

though *Saguinus* exhibits a characteristically small value among extant genera, the fossil specimen displays an even smaller value. The medial surface of the olecranon, from which *m. flexor digitorum profundus* originates, is somewhat concave in extant platyrrhines; however, a marked concavity as seen in *Neosaimiri* is only found in *Aotus*, *Saguinus*, and *Cebus*. The coronoid process (CRND/NTCH) of the fossil is moderately high like *Saimiri*, *Saguinus*, and *Pithecia*, but lower than those of *Cebus* and *Aotus* (Fig. 6, Table 4).

Femoral head and neck (Fig. 7)

Description. IGM-KU 89181 is a right femoral head associated with a partial neck, which is broken medial to the trochanteric fossa. The diameter of the head is 6.2 mm. The articular surface is shallow, covering less than a hemisphere, and extended slightly superoposteriorly towards the neck. The *fovea capitis femoris* is shallow and situated posteroinferiorly.

There is a sharp tubercle, to which the capsular ligament is attached, on the posterior aspect of the neck near the broken end (Fig. 7a). The tubercle is about 5 mm in length, 2 mm in width. The neck is moderately compressed anteroposteriorly. Although it is impossible to measure the whole length of the femoral neck, the neck seems short and stout, estimated by the position of the tubercle.

The other four isolated femoral heads (IGM-KU 89182, 89183, 89184, 89185) are similar to IGM-KU 89181 in size and shape of the articular surface. The head diameter ranges from 6.2 to 6.7 mm (Table 5, FHD). The average diameter of the five femoral heads is 6.42 mm (S.D. = 0.22).

Comparison. The average diameter of the fossil femoral heads is nearly the same as that of *Saimiri* (Table 5, FHD). Its shallow articular surface is shared with extant platyrrhines except *Pithecia*, which has a deeper articular surface with the larger extension on the superior aspect (also see Ford, 1980). Although a tubercle of the neck is usually present in the extant platyrrhines except *Cebus*, its size and shape are variable (Ford, 1980; Hershkovitz, 1988; Dagosto and Schmid, 1996). Among extant genera examined, it is large and sharp in *Saguinus*, large but obtuse in *Aotus*, and weakly developed in *Saimiri* and *Pithecia*. The condition of the fossil is intermediate between *Saguinus* and *Aotus*. The femoral neck (NCKD/FHD) is very thick as is in *Saguinus* almost beyond the ranges of other extant genera (Fig. 8, Table 5).

Distal femur (Fig. 9)

Description. There are three distal femur specimens, IGM-KU 89187, 89188, and 89189. IGM-KU 89187, a left distal epiphysis, is broken proximal to the patellar surface. The proximodistal length is about 11 mm. The epiphysis is crushed mediolaterally; thus, the bicondylar value is underestimated (Fig. 8, Table 6, BCDW). Taking account of the deformation, the epiphysis seems to be moderately narrow. The femoral condyles are weakly asymmetrical: the medial condyle protrudes slightly more distally and is more expanded externally than the lateral one, but the condylar widths are the

TABLE 4. Metric variables of the ulna

		OLCH	NTCH	OLCD	CRND	OLCH/ NTCH (%)	OLCD/ OLCH (%)	CRND/ NTCH[1] (%)
IGM-KU 89174		5.8	5.3	4.7	3.4	109.4	81.0	64.2
Saimiri	Mean	5.19	5.17	5.53	3.36	99.19	107.05	65.09
(n = 25)	S.D.	0.48	0.37	0.34	0.27	5.93	7.77	5.20
	Range	4.2–6.1	4.6–6.1	4.8–6.3	2.9–4.2	90.4–109.4	94.6–117.8	57.1–73.9
Aotus		5.81	6.06	6.20	3.44	95.67	105.45	67.3
(n = 19)		0.62	0.36	0.74	0.32	6.05	9.90	4.63
		4.6–7.0	5.5–6.7	5.3–7.5	2.8–4.2	79.0–104.5	82.0–119.1	46.2–63.3
Saguinus		4.74	4.09	4.33	2.65	109.81	94.79	64.22
(n = 16)		0.88	0.46	0.56	0.42	8.02	7.64	3.78
		3.6–6.7	3.3–4.8	3.4–5.3	2.0–3.5	92.7–118.9	81.0–104.3	56.8–70.3
Cebus		8.20	8.18	9.36	6.16	100.06	110.86	76.21
(n = 27)		0.94	0.80	0.73	0.85	10.57	7.54	9.04
		6.2–10.3	6.5–9.8	7.9–10.8	4.8–7.7	80.6–119.2	94.1–125.4	64.0–98.72
Pithecia		7.07	7.96	7.60	5.17	87.60	105.88	63.35
(n = 10)		1.11	0.75	0.85	0.40	10.73	8.05	5.15
		4.9–8.2	6.5–8.8	6.3–8.7	4.4–5.7	71.8–100.0	91.3–115.3	53.7–68.5

[1] Abbreviations: OLCH, height of the olecranon; NTCH, trochlear notch height; OLCD, anteroposterior diameter of the olecranon; CRND, height of the coronoid process (see Fig. 2).

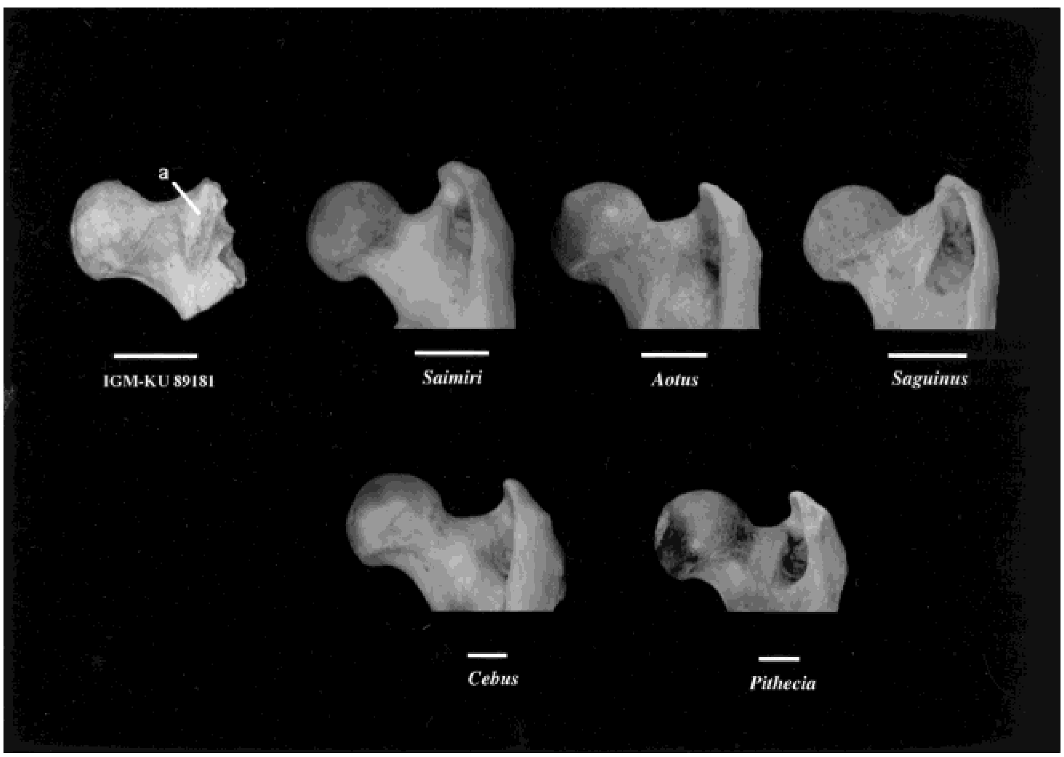

Fig. 7. Right proximal femora of *Neosaimiri* (IGM-KU 89181) and extant platyrrhines in posterior view. a = a sharp tubercle. Scales are changed to an approximately same size. Scale bars = 5 mm.

same (MCDW, LCDW). The patellar surface is well defined, although the medial lip is slightly damaged. The medial and lateral lips are moderately high, equally raised, and parallel (Fig. 9a). The patellar surface is narrow and modestly excavated.

IGM-KU 89188, a right distal epiphysis, is broken proximal to the patellar surface. The

TABLE 5. Metric variables of the proximal femur

		FHD	NCKD	NCKD/FHD[1] (%)
IGM-KU 89181		6.2	5.0	80.6
IGM-KU 89182		6.5	—	—
IGM-KU 89183		6.5	—	—
IGM-KU 89184		6.2	—	—
IGM-KU 89185		6.7	—	—
	Mean	6.42	—	—
Saimiri	Mean	6.62	4.95	74.73
(n = 25)	S.D.	0.36	0.39	3.21
	Range	6.0–7.8	4.4–6.3	68.7–80.8
Aotus		7.85	5.86	74.75
(n = 19)		0.39	0.33	4.16
		7.1–8.6	5.2–6.6	68.4–81.5
Saguinus		5.69	4.45	78.27
(n = 16)		0.72	0.56	3.38
		4.7–6.9	3.7–5.3	71.7–85.1
Cebus		10.56	7.70	72.93
(n = 27)		0.65	0.64	3.31
		9.5–12.0	6.4–9.0	66.0–80.4
Pithecia		10.51	7.89	75.10
(n = 10)		0.73	0.57	2.58
		9.2–11.3	7.0–8.7	71.4–80.4

[1] Abbreviations: FHD, diameter of the head; NCKD, diameter of the neck (see Fig. 2).

distal shaft is crushed along the medial patellar lip. The proximodistal length is about 12 mm. The overall size is the same as, but anteroposteriorly shallower than, IGM-KU 89187. The anteroposterior depth of the epiphysis is 87% of the bicondylar width (Table 6, DSTH/BCDW). The condition of the femoral condyles is similar to that of IGM-KU 89187. The medial condyle protrudes slightly distally, and expands externally. The posterior widths of the femoral condyles are the same. The width of the intercondylar notch is about 30% of the bicondylar width.

The patellar surface of IGM-KU 89188 is markedly asymmetrical, differing from IGM-KU 89187. Although the medial patellar lip is eroded along its whole length, it is apparent that the lateral lip is more raised than the medial one (Fig. 9b). The angle of the lateral slope of the patellar groove is very steep. The lateral to the patellar surface is so steep that the projection of the lateral epicondyle is emphasized. Although the patellar surface width must be estimated (Table 6, PTGW), the patellar surface of IGM-KU 89188 is narrow and remarkably deep differing from that of IGM-KU 89187.

IGM-KU 89189 is a left distal epiphysis which is broken proximal to the patellar surface. Since this specimen is badly crushed anteroposteriorly and mediolaterally, the width and depth can not be measured. The overall size seems slightly larger than that of IGM-KU 89187 and 89188 although this impression may be biased. The condylar widths are close to those of other two fossils. The medial condyle is slightly wider than the lateral condyle.

The patellar surface is crushed as a whole and the medial lip is eroded. But only the proximal part of the lateral lip is preserved. The lateral lip is well raised, but not emphasized as much as in IGM-KU 89188. The lateral side of the lateral lip is sloped moderately as compared with IGM-KU 89188. In these regards, this specimen shows an affinity to IGM-KU 89187.

Comparison. The overall size of the fossil specimens is smaller than that of *Saimiri*, and subequal to that of *Saguinus* (Table 6, BCDW, DSTH). The depth to width ratio of the epiphysis (DSTH/BCDW) is extraordinally large in IGM-KU 89187. But, this is a bias due to the underestimation of BCDW of IGM-KU 89187. IGM-KU 89188 is moderately deep anteroposteriorly (DSTH/BCDW) resembling *Aotus*, *Saimiri* and *Saguinus* have a somewhat deeper and *Cebus* and *Pithecia* a shallower epiphysis (Fig. 8, Table 6). Although it is a rough impression, IGM-KU 89187 seems to be somewhat deeper than IGM-KU 89188 even if it is intact.

The femoral condyles are less asymmetrical in the fossils (Fig. 8, Table 6, LCDW/MCDW). Although the condylar widths are somewhat more asymmetrical in IGM-KU 89189, the average of the ratio in fossils (97.2) is intermediate of those between *Saimiri* and *Aotus*. Other extant genera demonstrate a more broadened medial condyle.

The morphology of the patellar surface varies among the fossils. IGM-KU 89187, in which the patellar lips are parallel and modestly raised, is similar to *Saimiri*, *Aotus*, and *Saguinus*. The elevation of the lateral lip in IGM-KU 89189 also resembles the condition in IGM-KU 89187 and these extant taxa. By contrast, the patellar surface of IGM-KU 89188 exhibits a more asymmetrically raised lateral lip. This condition some-

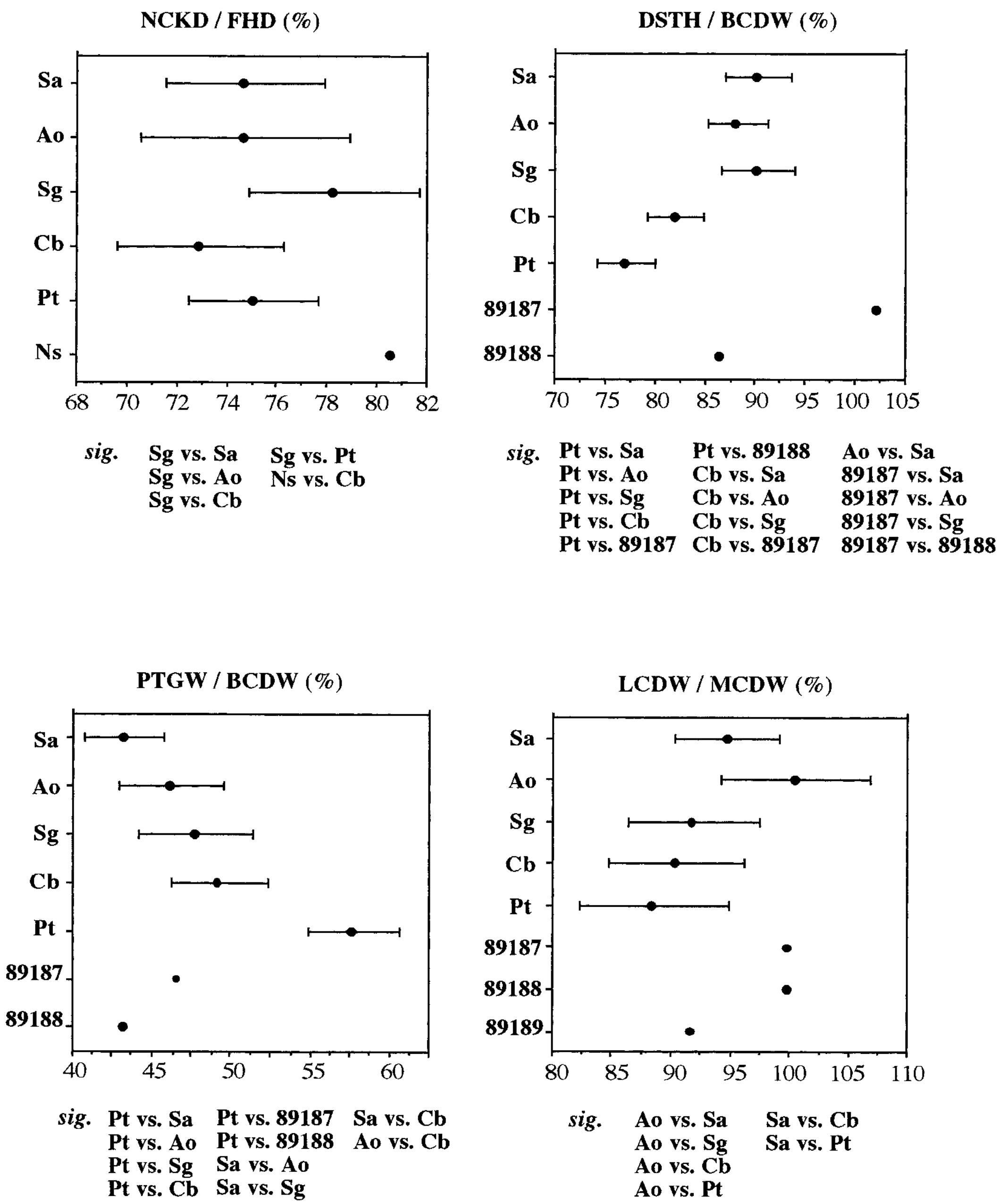

Fig. 8. Mean and ±1 standard deviation of femoral variables. Statistical difference was tested for by multiple comparison (Fisher's PLSD) at $P = 0.05$ and significantly different pairs are shown below each plot. For species name, see Figure 4. BCDW of IGM-KU 89187 is underestimated due to deformation.

what resembles those of *Cebus* and *Pithecia*, although the lateral lip is further more emphasized in the fossil. The patellar surface of IGM-KU 89188 is very deep like that of *Cebus*. As for the patellar surface width, however, all of the fossils exhibit a narrow condition resembling *Saimiri, Aotus,* and *Saguinus*.

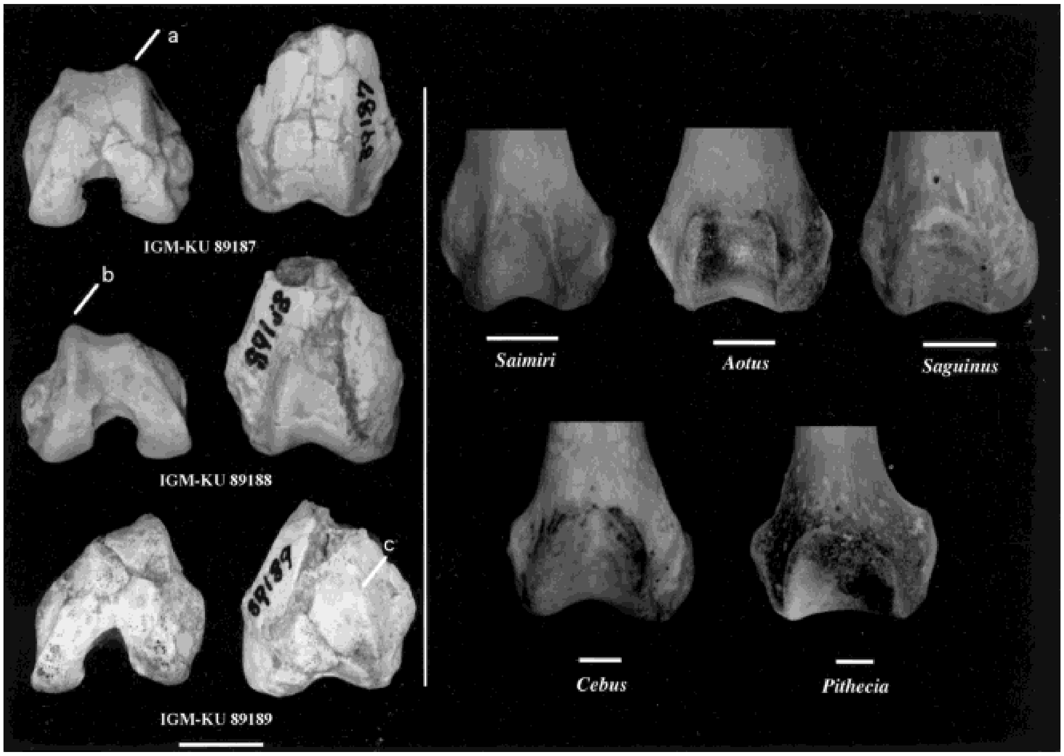

Fig. 9. Distal femora of *Neosaimiri* (upper: IGM-KU 89187; middle: IGM-KU 89188; lower: IGM-KU 89189) and extant platyrrhines (all right femur) in anterior view. For *Neosaimiri*, a distal view is also shown. a, b, c = lateral lips. Scales are changed to an approximately same size. Scale bars = 5 mm.

Distal tibia (Fig. 10)

Description. There are two new distal tibiae: IGM-KU 89194 and 89195, and a previously described specimen, IGM 250406 (Meldrum and Kay, 1997). IGM-KU 89194 is a 12-mm-long fragment of left distal tibia lacking the medial malleolus. The mediolateral breadth is moderately wider that the anteroposterior length (Table 7, TBAP/TBML). The distal surface is slightly concave anteroposteriorly. The median ridge is low as a whole and faint at the center of the surface. The ridge runs anterolaterally and continues to a small beak on the anterior border of the distal surface (Fig. 10a). On the medial side of the anterior beak, there is a small articular facet extended from the distal surface along the anterior border (Fig. 10b). This facet does not extend onto the anterior surface of the shaft.

The posterior surface of the distal shaft is flat. At the base of the medial malleolus, there is a narrow groove for the tendon of *m. tibialis posterior.* The groove for the tendon of *m. flexor hallucis longus* is indistinct. On the lateral surface of the shaft, there is a smooth semilunar notch for the fibula, which is continuous with the distal articular surface (Fig. 10c). The anteroposterior length of the fibular notch is about two-thirds of the lateral surface. The anterior surface of this facet is roughened for the anterior inferior tibiofibular ligaments. Posteriorly, there is an ascending ridge, in which the posterior inferior tibiofibular ligament is attached. A triangular flat surface is present proximal to the fibular notch. The posterior ridge continues proximally to the interosseous ligament crest (Fig. 10d).

IGM-KU 89195 is a 10-mm-long fragment of right distal tibia including the medial malleolus. The overall size and morphology are quite similar to those of IGM-KU 89194. The medial malleolus is long and slender

TABLE 6. Metric variables of the distal femur

		BCDW	MCDW	LCDW	DSTH	PTGW	DSTH/ BCDW (%)	PTGW/ BCDW (%)	LCDW/ MCDW[1] (%)
IGM-KU 89187		9.0[2]	3.4	3.4	9.2	4.2	102.2[2]	46.7[2]	100.0
IGM-KU 89188		9.7	3.4	3.4	8.4	(4.2)[3]	86.6	(43.3)[3]	100.0
IGM-KU 89189		—	3.6	3.3	—	—	—	—	91.7
Saimiri	Mean	11.20	3.79	3.61	10.12	4.85	90.27	43.23	94.79
(n = 25)	S.D.	0.54	0.24	0.29	0.57	0.39	3.35	2.53	4.47
	Range	10.3–12.7	3.4–4.3	3.1–4.2	8.8–11.3	4.1–5.7	85.4–98.2	38.7–49.6	88.6–102.6
Aotus		13.29	4.44	4.55	11.73	6.14	88.22	46.20	100.57
(n = 19)		0.47	0.26	0.35	0.66	0.55	2.99	3.26	6.28
		12.4–14.0	4.1–5.1	4.0–5.1	10.4–12.9	5.2–7.6	80.6–92.4	41.3–54.7	88.9–109.3
Saguinus		9.07	3.29	3.00	8.20	4.36	90.33	42.80	91.92
(n = 16)		0.75	0.29	0.27	0.82	0.50	3.65	3.58	5.55
		8.0–10.0	2.9–3.8	2.6–3.5	7.0–9.5	3.8–5.6	85.4–96.7	41.5–52.4	80.0–100.0
Cebus		18.57	6.65	6.14	15.29	9.11	82.09	49.26	90.50
(n = 27)		1.72	0.85	0.73	1.20	0.99	2.84	3.06	5.71
		15.9–22.3	5.2–8.4	5.0–7.9	13.4–17.8	7.5–11.0	75.9–87.7	44.6–54.9	80.6–98.2
Pithecia		17.78	6.54	5.79	13.72	10.39	77.14	57.72	88.63
(n = 10)		0.76	0.46	0.48	0.84	0.81	2.90	2.88	6.26
		16.6–18.9	6.0–7.3	4.8–6.4	12.2–14.6	9.4–12.0	73.5–81.4	52.2–61.9	79.5–100.0

[1] Abbreviations: BCDW, bicondylar width; MCDW, width of the medial condyle; LCDW, width of the lateral condyle; DSTH, anteroposterior depth of the distal epiphysis; PTGW, width of the patellar groove (see Fig. 2).
[2] Affected by deformation.
[3] Estimation.

TABLE 7. Metric variables of the distal tibia

		TBAP	TBML	TBAP/TBML[1] (%)
IGM-KU 89194		5.8	6.9	84.1
IGM-KU 89195		5.8	6.8	85.3
IGM 250436 (cast)		5.8	7.0	82.9
	Mean	5.80	6.90	84.50
Saimiri	Mean	6.32	7.32	84.33
(n = 25)	S.D.	0.32	0.46	3.95
	Range	5.4–6.9	6.2–8.3	75.0–91.9
Aotus		7.58	8.73	85.60
(n = 19)		0.60	0.62	3.85
		6.6–8.5	7.8–10.0	77.5–92.4
Saguinus		5.02	5.81	84.50
(n = 16)		0.50	0.60	5.68
		4.2–5.8	5.0–7.1	73.4–90.3
Cebus		9.77	12.27	77.85
(n = 27)		0.91	1.01	3.84
		8.4–12.4	10.8–14.0	69.6–84.6
Pithecia		8.88	11.76	74.32
(n = 10)		0.33	0.90	4.23
		8.3–9.3	10.2–12.9	68.0–79.8

[1] Abbreviations: TBAP, anteroposterior length of the distal epiphysis; TBML, mediolateral width of the distal epiphysis (see Fig. 2).

(2.7 mm in length, 4.0 mm in anteroposterior width at the base). The inner (lateral) surface of the malleolus makes a right angle with respect to the distal articular surface. At the distal end of the malleolus, there is a marked sulcus for the deltoid ligament. The posterior base of the medial malleolus forms a shallow groove for the tendon of *m. tibialis posterior*. The distal surface displays similar features to IGM-KU 89194: weak anteroposterior convexity, a low median ridge, a small anterior beak, and a small articular facet on the anterior border. The posterior surface of the epiphysis is flat. The lateral surface has a smooth semilunar fibular notch. As is in IGM-KU 89194, there are well-developed insertions for the inferior tibiofibular ligaments adjacent to the fibular notch.

Meldrum and Kay (1997) describe a distal fragment of left tibia, IGM 250406. Its size and morphology are very similar to both IGM-KU 89194 and 89195. However, its fibular notch is rugose, differing from the smooth condition of the specimens described here.

Comparison. The overall size of the fossils is slightly smaller than the average *Saimiri* (Table 7, TBAP, TBML). The epiphysis is moderately wide like *Saimiri*, *Aotus*, and *Saguinus*, and much narrower than *Cebus* and *Pithecia* (Fig. 11, Table 7, TBAP/TBML). Although the morphology of the fibular notch is uniform in the fossil and living platyrrhines, the development of the inferior tibiofibular ligament insertions, particularly that of the posterior ligament, is quite variable. The insertions are well developed in the fossils and *Saimiri* while it is poorly developed in *Aotus* and *Cebus*. *Pithe-*

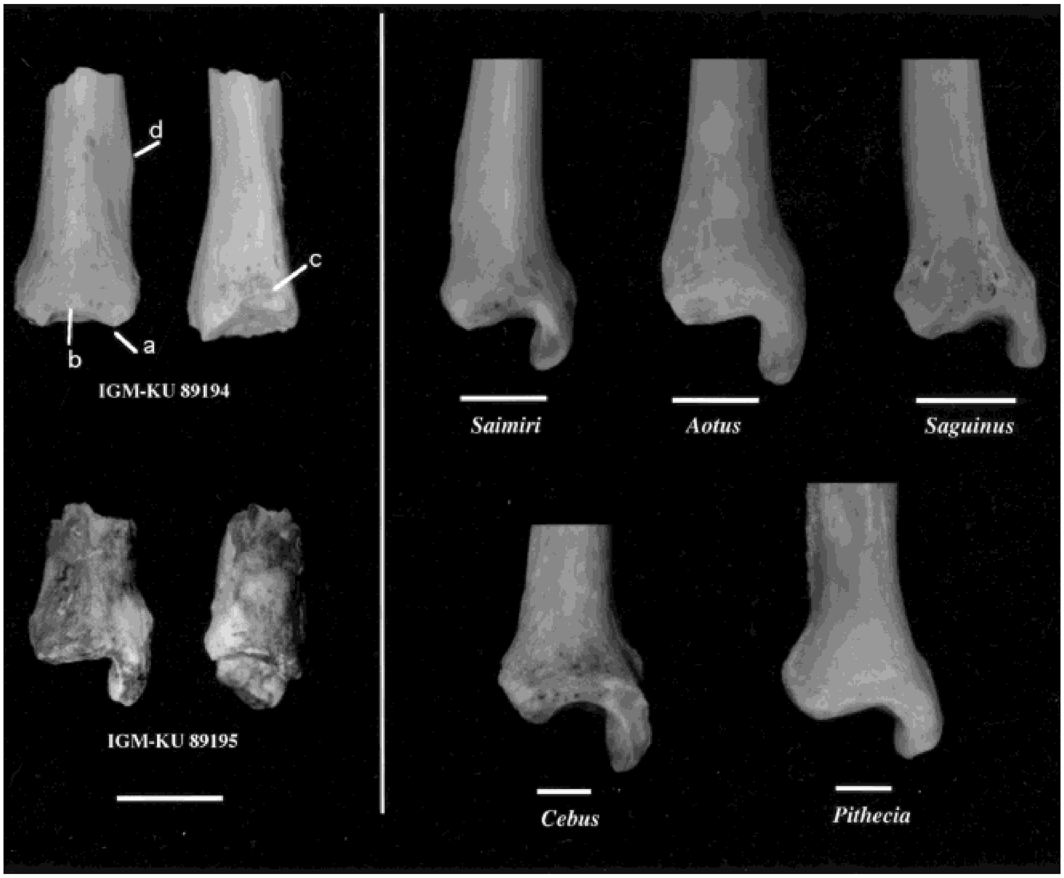

Fig. 10. Distal tibiae of *Neosaimiri* (upper: IGM-KU 89194; lower: IGM-KU 89195) and extant platyrrhines (all right tibia) in anterior view. IGM-KU 89194, a left tibia, lacks the medial malleolus. For *Neosaimiri,* a lateral view is also shown (right in the left panel). a = a small beak; b = a small articular surface; c = a smooth semilunar notch; d = a posterior edge. Scales are changed to an approximately same size. Scale bars = 5 mm.

cia is unique in its remarkably developed insertions and interosseous ligament crest.

The size of the beak on the anterior border of the distal surface is relatively small in the fossils. This condition resembles that of *Aotus*. *Saimiri, Saguinus,* and in particular *Cebus* exhibit a more salient beak. The facet on the anterior border of the distal surface is commonly observed in the fossil specimens and extant genera. This facet is not expanded further on the anterior aspect of the shaft in the fossils and many specimens of *Aotus* and *Cebus.* On the contrary, there is an anterior extension of the facet in the most specimens of *Saimiri* and *Pithecia*, and in the majority of the *Saguinus* specimens (but also see Ford, 1980).

Talus (Fig. 12)

Description. There are three new fossil tali (IGM-KU 89030, 89031, and 89199) and a previously described talus (IGM-KU 88003). IGM-KU 89030 is a left talus with the proximal trochlea broken. The trochlea width is 4.6 mm. The trochlea is quadrilateral in dorsal view and moderately concave. The trochlea is nearly symmetrical: both lateral and medial lips are similarly sharp and high although the lateral lip is somehow more acute and the lateral slope of the trochlear groove is slightly steeper than the medial one. The trochlear lips protrude more distally than the midtrochlea surface. The most distal part of the midtrochlea surface is flat rather than depressed (Fig. 12a). The

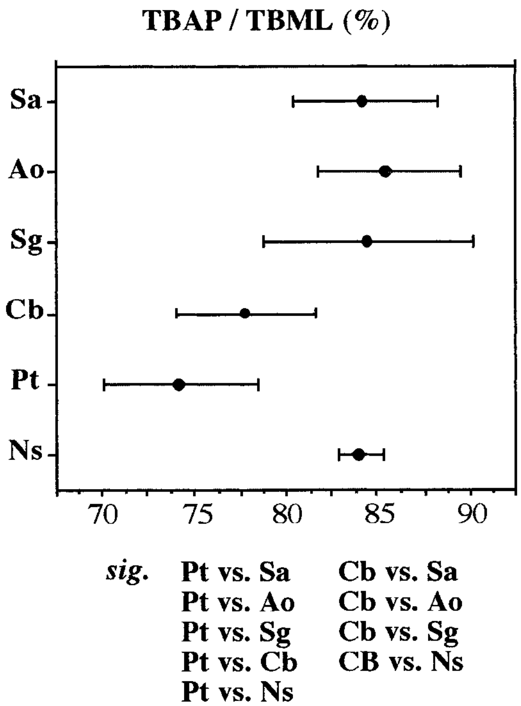

Fig. 11. Mean and ±1 standard deviation of tibial variable. Statistical difference was tested for by multiple comparison (Fisher's PLSD) at $P = 0.05$ and significantly different pairs are shown below each plot. For species name, see Figure 4.

talar body is moderately narrow and long (Table 8, TRCW/TRCL). The medial and lateral walls of the trochlea are steep. The tibial and fibular malleolar facets are relatively small and shallow. The talar neck (including the head) is long, flexed slightly plantarward and angled medially at about 45°. The head is modestly compressed dorsoplantarly (THDH/THDW) and rotated slightly.

IGM-KU 89031 is a complete left talus. The trochlea is 4.9 mm in width and 6.0 mm in length. Although the overall size slightly exceeds that of IGM-KU 89030, both specimens are quite similar in shape. The trochlea width is 81.7% of the length (TRCW/TRCL). The trochlea lips are parallel and sharp. The trochlear surface is weakly grooved with a flat distal midtrochlea surface. The side walls of the trochlea are vertical and both tibial and fibular malleolar facets are small and shallow. The proximal medial tubercle, where the posterior tibiotalar ligament is attached, is moderately large and directed plantarward. The groove for *m. flexor hallucis longus* is wide and shallow. The talar neck length including the talar head is 80% of the trochlea length (NCKL/TRCL). The head size (THDW/TRCW), head shape (THDH/THDW), and the degree of rotation do not differ significantly from those of IGM-KU 89030.

IGM-KU 89199 is an almost complete right talus. The anterior end of the proximal calcaneal surface is broken. The overall size is slightly larger than the other two specimens: the trochlea is 5.0 mm in width and 6.4 mm in length. However, it exhibits very similar morphology to IGM-KU 89030 and 89031. The trochlear lips are parallel and similar in height. The trochlea surface is modestly concave. The distal midtrochlea surface is nearly flat. In its proportions, the trochlea is slightly narrower than that of IGM-KU 89031 (TRCW/TRCL). The side walls of the trochlea are steep and the malleolar facets are small and shallow. The medial tubercle is moderately large and the groove for *m. flexor hallucis longus* is distinct. The relative neck length (NCKL/TRCL) is the same as in IGM-KU 89031. In the relative head size (THDW/TRCW) and head height (THDH/THDW) IGM-KU 89199 has similar values as IGM-KU 89030.

Gebo et al. (1990) described a complete right talus, IGM-KU 88003 (=8803), which was collected at the same locality in 1988 (Fig. 12). This specimen is similar to IGM-KU 89030 in size and is slightly smaller than IGM-KU 89031 and 89199. The relative trochlear width (TRCW/TRCL) is almost the same as the present specimens. Although the trochlea lips are somehow sharper, IGM-KU 88003 shares the following morphological features with the present specimens: parallel trochlea lips, a flat midtrochlea, a shallow tibial malleolar facet, a weak lateral flare of the fibular facet, and a tightly curved medial tubercle (Gebo et al., 1990). Although the neck is proportionally longer than that of IGM-KU 89031 and 89199 (NCKL/TRCL), the absolute value (NCKL) is smaller than that of similar-sized IGM-KU 89030 (in which the TRCL can not be measured). The relative head width (THDW/TRCW) and relative head height (THDH/THDW) are within the ranges of the new fossils.

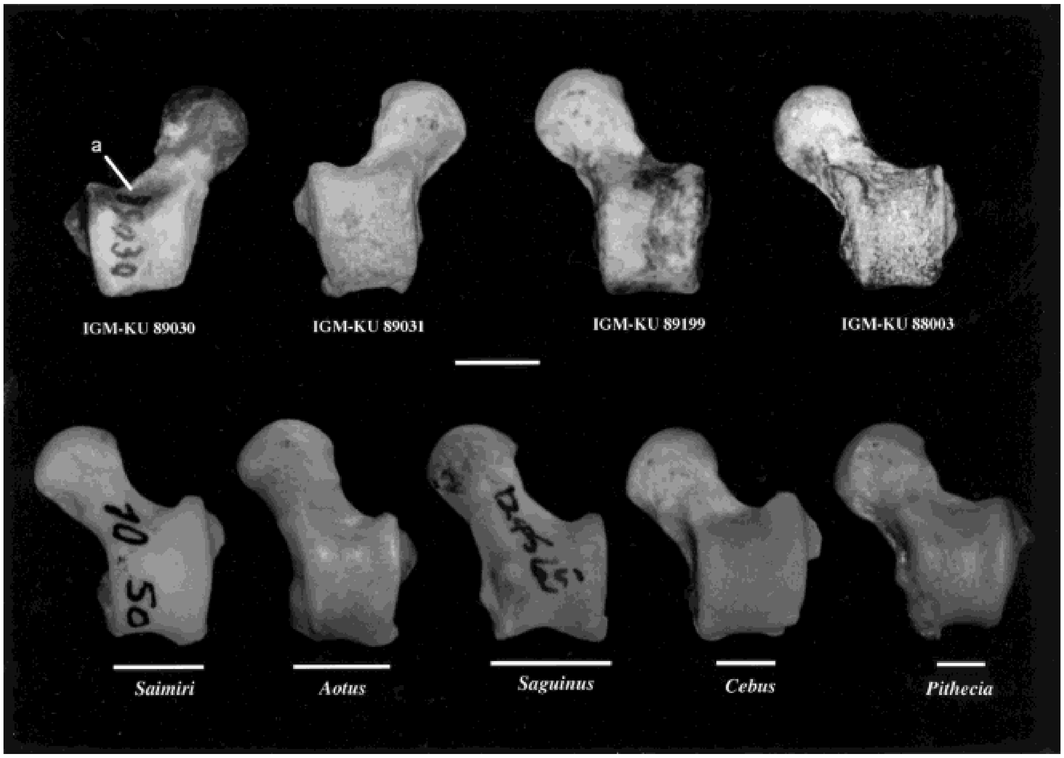

Fig. 12. Tali of *Neosaimiri* (from left to right: IGM-KU 89030, 89031, 89199, 88003) and extant platyrrhines in dorsal view. a = flat distal surface of the midtrochlea. Scales are changed to an approximately same size. The photograph of *Saguinus* is reversed to the right for comparative purposes. Scale bars = 5 mm.

Comparison. The overall size of the four fossil tali lies within the range of *Saimiri,* and below that of *Aotus* (Table 8, TRCW, TRCL). The proportion of the trochlea of the fossils is moderately narrow and close to those of *Saimiri* and *Cebus* (Fig. 13, Table 8, TRCW/TRCL). The trochlea of *Aotus* is narrower and that of *Saguinus* and *Pithecia* is wider. The quadrilateral trochlear form in the fossils is common with extant genera except *Pithecia,* in which the medial lip is more medially angled. The fossil specimens as well as *Aotus, Saguinus,* and *Pithecia* have a flat distal midtrochlea surface. By contrast, *Saimiri* and *Cebus* exhibit a marked depression. The steep side walls of trochlea and shallow tibial and fibular malleolar facets resemble the conditions in *Saimiri, Aotus,* and *Saguinus.* Differing from this, the medial and lateral side walls of the trochlea are obliquely angled in *Pithecia* and the tibial malleolar facet is large and deeply concave being extended onto the neck in *Cebus.*

The talar neck of the fossils is moderately long. The proportion is most close to the average of *Saimiri* (NCKL/TRCL). Although the ranges of *Aotus* and *Cebus* overlap that of the fossils, averages are somewhat higher and lower, respectively. The talar head of the fossils is small like *Saimiri* and *Saguinus* (THDW/TRCW). Other extant genera, particularly *Aotus,* exhibit larger values although this trait is highly variable. The talar head of the fossils is moderately flattened as much as in *Aotus* and *Saguinus* (THDH/THDW). The talar head is less flattened in the other extant genera.

Calcaneus (Fig. 14)

Description. IGM-KU 89202 is a complete left calcaneus. The whole length is 15.5 mm. The height of the calcaneus is 34.2% of the whole length (Table 9, CALH/CALL).

TABLE 8. Metric variables of the talus

		TRCW	TRCL	NCKL	THDW	THDH	TRCW/ TRCL (%)	NCKL/ TRCL (%)	THDW/ TRCW (%)	THDH/ THDW[1] (%)
IGM-KU 89030		4.6	—	5.1	4.3	3.4	—	—	93.5	79.1
IGM-KU 89031		4.9	6.0	4.8	4.5	3.5	81.7	80.0	91.8	77.8
IGM-KU 89199		5.0	6.4	5.1	4.7	3.8	78.1	79.7	94.0	80.9
IGM-KU 88003		4.5	5.7	4.8	4.3	3.4	79.0	84.2	95.6	79.1
	Mean	4.75	6.07	4.95	4.45	3.53	79.60	81.30	93.73	79.22
Saimiri	Mean	4.77	6.30	5.09	4.53	3.76	77.15	81.45	92.19	83.54
(n = 25)	S.D.	0.26	0.38	0.34	0.27	0.26	3.43	5.93	3.73	4.15
	Range	4.3–5.4	5.6–7.1	4.6–6.1	4.0–5.1	3.3–4.6	70.8–83.1	72.3–95.2	85.2–97.9	77.8–90.2
Aotus		5.44	7.41	6.12	5.45	4.27	74.47	83.55	100.21	78.37
(n = 16)		0.27	0.46	0.43	0.29	0.23	3.05	4.36	4.92	2.96
		4.9–5.9	6.7–8.1	5.5–7.0	5.1–5.9	4.0–4.8	70.0–80.6	77.2–90.0	91.5–105.9	72.4–83.3
Saguinus		3.94	4.27	3.88	3.76	2.94	93.08	88.88	93.10	78.17
(n = 12)		0.42	0.45	0.50	0.36	0.36	3.34	6.89	5.32	5.17
		3.4–4.9	3.6–5.0	2.8–4.6	3.0–4.3	2.3–3.4	88.0–98.0	76.7–97.6	84.4–100.0	69.4–85.0
Cebus		8.14	10.26	8.06	7.92	6.56	79.56	78.65	95.66	83.10
(n = 16)		0.45	0.85	0.57	0.83	0.57	3.63	3.61	5.24	4.07
		7.3–9.1	9.1–12.1	7.0–9.4	6.6–9.1	6.6–7.8	74.1–85.7	73.4–84.5	88.6–103.6	73.7–89.4
Pithecia		7.79	9.41	7.00	7.45	5.76	82.76	75.76	95.88	76.10
(n = 8)		0.39	0.35	0.74	0.51	0.45	2.65	4.01	5.00	2.71
		7.2–8.3	8.7–9.7	5.4–8.0	6.6–8.0	5.1–6.4	77.4–85.6	70.8–83.3	90.2–103.9	71.2–79.4

[1] Abbreviations: TRCW, width of the trochlea; TRCL, length of the trochlea; NCKL, length of the neck and head; THDW, width of the talar head; THDH, height of the talar head (see Fig. 2).

The width of the body of the calcaneus is 31.0% of the length (CALW/CALL). The calcaneal tuberosity is relatively long. The length of the calcaneal tuberosity is 64.5% of the distal calcaneal length (HEEL/DSTL). The tuberosity is mediolaterally narrow and inclined laterally at about 45°. The proximal facet is long (about 34% of the whole length), narrow, and slanted medially. The sustentaculum tali is small. The sustentaculum is short, being about 20% of the length of the calcaneus. On the plantar side of the sustentaculum, there is a modestly deep groove for *m. flexor hallucis longus*. The peroneal tubercle is large and expanded laterally. The medial facet of the subtalar joint is small and continuous with the anterior facet by a strip of smooth surface. The distal facet is modestly large and inclined dorsally distally. The calcaneocuboid facet is semilunar-shaped and modestly concave.

IGM-KU 89203 is a complete left calcaneus. Although there are minor morphological differences from IGM-KU 89202, two fossil calcaneus quite resemble each other. The whole length is 15.9 mm. The calcaneal height and width are nearly equal with those of IGM-KU 89202. The load-to-power arm ratio of the triceps surae (HEEL/DSTL) is somehow smaller as compared with IGM-KU 89202. The sustentaculum is as short as in IGM-KU 89202. The groove for *m. flexor hallucis longus* is slightly deeper. The peroneal tubercle is modestly large, although it is smaller than that of IGM-KU 89202. The morphologies of the proximal, medial and distal facets of the subtalar joint, and calcaneocuboid facet are similar to those of IGM-KU 89202.

Comparison. The overall size of the fossil calcanei is equivalent to that of *Saimiri* (Table 9, CALL, CALW). The overall shape most resembles that of *Saimiri* (Fig. 15, Table 9, CALH/CALL, CALW/CALL). The body of calcaneus is wider in *Aotus*, taller and narrower in *Saguinus*, taller and wider (or shorter) in *Cebus*, and taller in *Pithecia*. The length of the calcaneal tuberosity (HEEL/DSTL) is close to that of *Aotus* and *Saguinus*. It is smaller in *Saimiri* and larger in *Cebus* and *Pithecia*.

The proximal facet of the fossil calcanei, which is narrow and long, and moderately inclined, resembles that of extant platyrrhines excluding *Cebus*. The facet of *Cebus* exhibits a shortness and distinctively steep angulation. The length of the sustentaculum tali of the fossils is similar to that of extant platyrrhines. There is no substantial variation in the sustentaculum length. However, the medial facet is not large in the fossils as

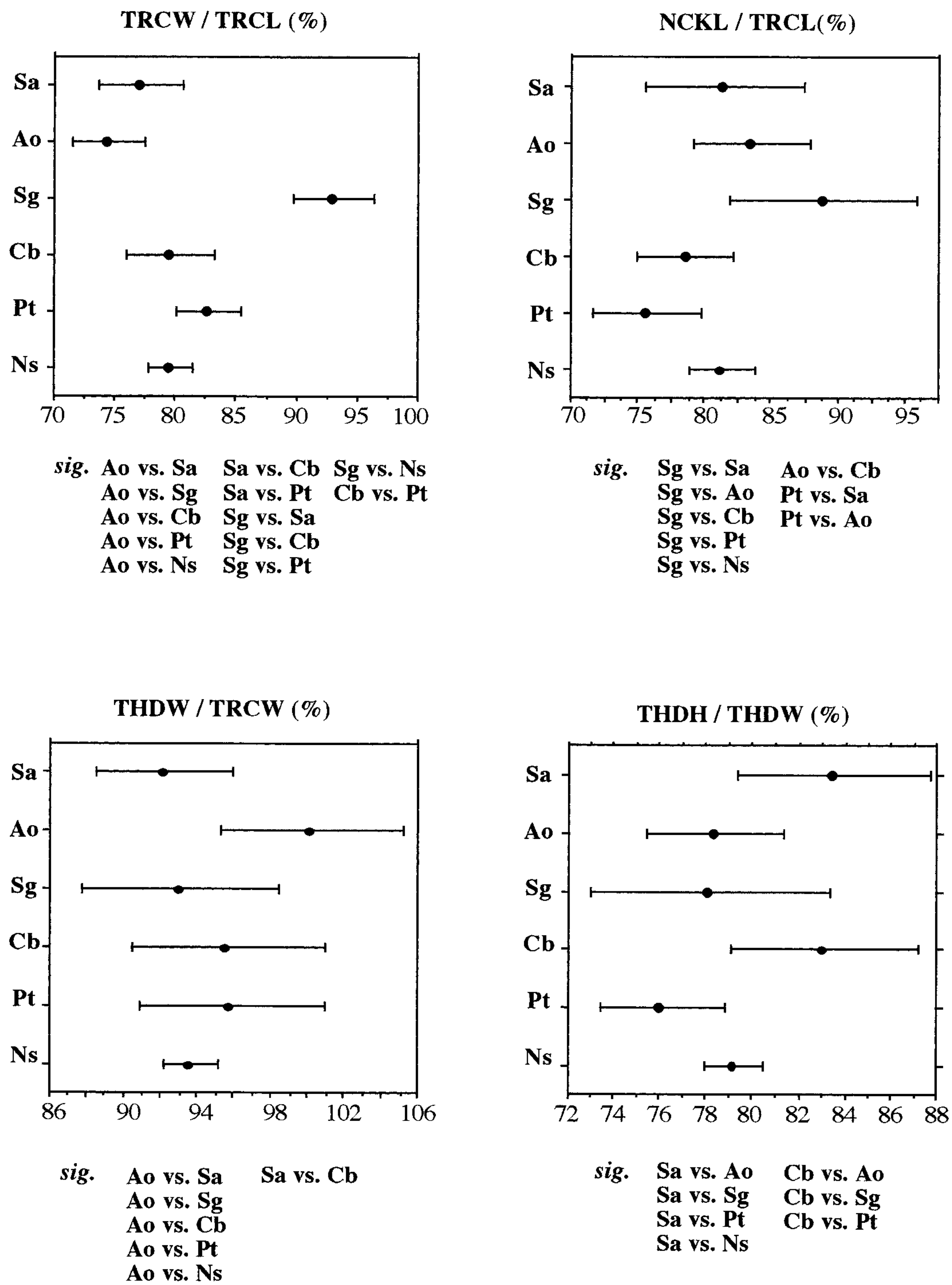

Fig. 13. Mean and ±1 standard deviation of talar variables. Statistical difference was tested for by multiple comparison (Fisher's PLSD) at $P = 0.05$ and significantly different pairs are shown below each plot. For species name, see Figure 4.

TABLE 9. Metric variables of the calcaneus

		CALL	HEEL	CALH	CALW	DSTL	SSTC	CALH/ CALL (%)	CALW/ CALL (%)	HEEL/ DSTL (%)	SSTC/ CALL[1] (%)
IGM-KU 89202		15.5	4.0	5.3	4.8	6.2	3.1	34.2	31.0	64.5	20.0
IGM-KU 89203		15.9	3.9	5.6	4.8	6.6	3.1	35.2	30.2	59.1	19.5
	Mean	15.70	3.95	5.45	4.80	6.40	3.10	34.70	30.60	61.80	19.75
Saimiri	Mean	16.00	3.78	5.82	4.82	7.05	3.51	36.41	30.00	51.80	21.80
(n = 25)	S.D.	0.74	0.43	0.28	0.44	0.42	0.48	1.45	2.24	4.56	2.69
	Range	14.9–17.6	3.0–4.7	5.3–6.3	4.1–5.6	6.3–7.9	2.2–4.2	34.3–40.5	26.2–33.5	42.9–59.4	14.8–25.2
Aotus		18.47	4.62	6.56	7.04	7.61	4.41	35.56	37.36	58.42	23.42
(n = 16)		0.75	0.69	0.34	0.50	0.38	0.48	1.19	2.35	8.21	2.21
		17.3–19.9	3.4–5.9	5.6–7.2	6.4–7.6	7.1–8.2	2.2–4.2	33.3–37.8	33.9–40.2	46.6–70.4	19.6–26.3
Saguinus		11.97	2.92	4.64	3.30	5.07	2.55	38.80	27.95	59.45	21.62
(n = 12)		1.04	0.29	0.49	0.35	0.37	0.29	1.43	1.55	5.10	2.08
		10.6–14.0	2.6–3.4	4.0–5.6	2.8–4.2	4.6–6.0	2.1–3.2	36.2–41.3	25.4–30.2	51.0–69.4	17.7–24.5
Cebus		25.25	7.32	9.52	9.19	10.11	5.64	38.02	36.60	70.74	22.41
(n = 16)		1.87	0.66	0.81	0.83	0.90	0.63	2.27	2.60	6.74	1.56
		22.5–29.6	5.9–8.7	8.2–10.7	8.0–11.0	8.2–11.9	4.7–6.8	34.2–42.9	30.6–42.0	60.9–80.6	19.9–25.4
Pithecia		23.02	6.14	9.30	7.6	8.69	5.7	39.86	31.43	73.35	22.67
(n = 8)		1.32	1.25	1.01	0.34	0.72	0.21	3.53	1.22	10.38	2.14
		20.9–24.7	4.0–7.6	8.0–10.7	7.4–7.9	7.4–9.9	5.2–6.1	34.4–45.3	29.0–33.0	55.7–84.4	18.1–24.6

[1] Abbreviations: CALL, length of the calcaneus; HEEL, length of the calcaneal tuberosity; CALH, height of the calcaneus; CALW, width of the calcaneus; DSTL, length of the distal calcaneus; SSTC, length of the sustentaculum tali (see Fig. 2).

well as *Saimiri*, *Aotus*, and *Saguinus* as compared to *Cebus* and *Pithecia*. The calcaneocuboid facet is kidney or semilunar shaped and modestly concave in all extant genera examined.

Statistical comparisons

Figures 4, 6, 8, 11, 13, and 15 graphically portray the outcome of Fisher's PLSD tests for humeral, ulnar, femoral, tibial, talar and calcaneal variables, respectively. Plots of the species' means and standard deviations allow visual display of known variation in extant taxa in comparison with our fossil specimens. There is great morphological variation in three fossil femoral specimens. (Fig. 8).

DISCUSSION

Taxonomical identification

The postcranial fossils described above were discovered in a very small locality together with dental specimens, which were identified as *Neosaimiri fieldsi* (Takai, 1994). Both dental and postcranial remains, moreover, are included the same size category as that of *Saimiri*. Furthermore, the postcranial fossils exhibit morphological uniformities (femoral head, distal tibia, talus, and calcaneus) and a consistent functional signal, which is generally common with *Saimiri* (see below). Therefore, it is most reasonable to presume these fossils represent a single taxon, *N. fieldsi*.

However, three distal femur specimens are exceptional in presenting great morphological variation (Fig. 8, Table 6). In IGM-KU 89187, the medial and lateral patellar lips are equally raised and the patellar surface is moderately deep, while the lateral lip of IGM-KU 89188 is markedly elevated more than the medial one, and the patellar surface is deeper. Although IGM-KU 89189 is badly crushed, the intact part of the lateral patellar lip shows an affinity to IGM-KU 89187. Concerning the morphology of the patellar surface, IGM-KU 89188 is very different from not only IGM-KU 89187 and 89189, but also extant platyrrhines.

Two interpretations of this variation are possible. First, IGM-KU 89188 represents a different genera from the other two fossils. In this case, these fossils may be attributed separately to either *Neosaimiri* or "*Laventiana*," splitting the *Saimiri*-like platyrrhine in La Venta as advocated by Rosenberger et al. (1991a). The weakness of this interpretation is the small variability of the other postcranial remains (i.e., femoral head, distal tibia, talus, and calcaneus). If the marked difference of the knee morphology is related to generic level different locomotor repertoires (indeed, the patellar surface of IGM-KU 89188 is unique as compared with

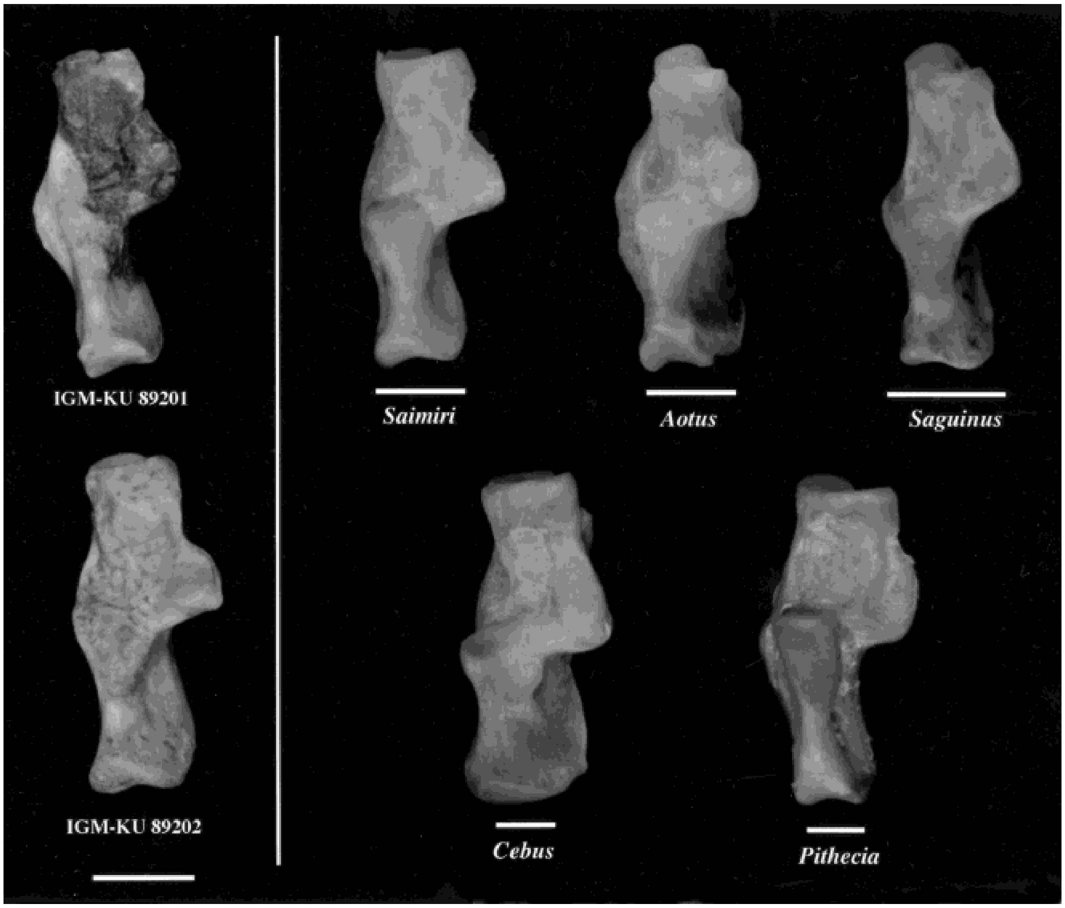

Fig. 14. Left calcanei of *Neosaimiri* (upper: IGM-KU 89201; lower: IGM-KU 89202) and extant platyrrhines in dorsal view. Scales are changed to an approximately same size. Scale bars = 5 mm.

extant platyrrhines), it would be reasonable to expect two morphotypes in other hindlimb regions. The fossil assemblage from the Masato Site is presumed to represent 10 or 11 individuals including at least four juveniles (Takai, 1994 and personal communication). If these three distal femora represent two taxa, why do not other postcranial remains do so? Or, are these two taxa very similar except for the patellar surface morphology?

Alternatively, this morphological difference might represent intraspecific variation of *Neosaimiri*. Although those specimens are very different in the shape of the lateral patellar lip, in other features (e.g., general size, condylar shape) they are similar to each other. One of the two types (e.g., IGM-KU 89188) may represent an extreme in the morphological variation of the patellar surface. However, this is not very convincing. While there is a great variation in the shape of the patellar surface in extant *Saimiri* (Fig. 16) and somewhat similar morphotypes like IGM-KU 89188 (right) and 89187 (left) are found, the morphological variability in 25 *Saimiri* individuals does not reach that found in only three fossils.

In conclusion, both interpretations are still inconclusive. However, the evidence seems insufficient to split these specimens into different taxa. Further specimens, especially of the distal femur, are needed to reach a firm conclusion. In the following sections we refer to IGM-KU 89187 and IGM-KU 89189 as the patellar surface morphology of *Neosaimiri*.

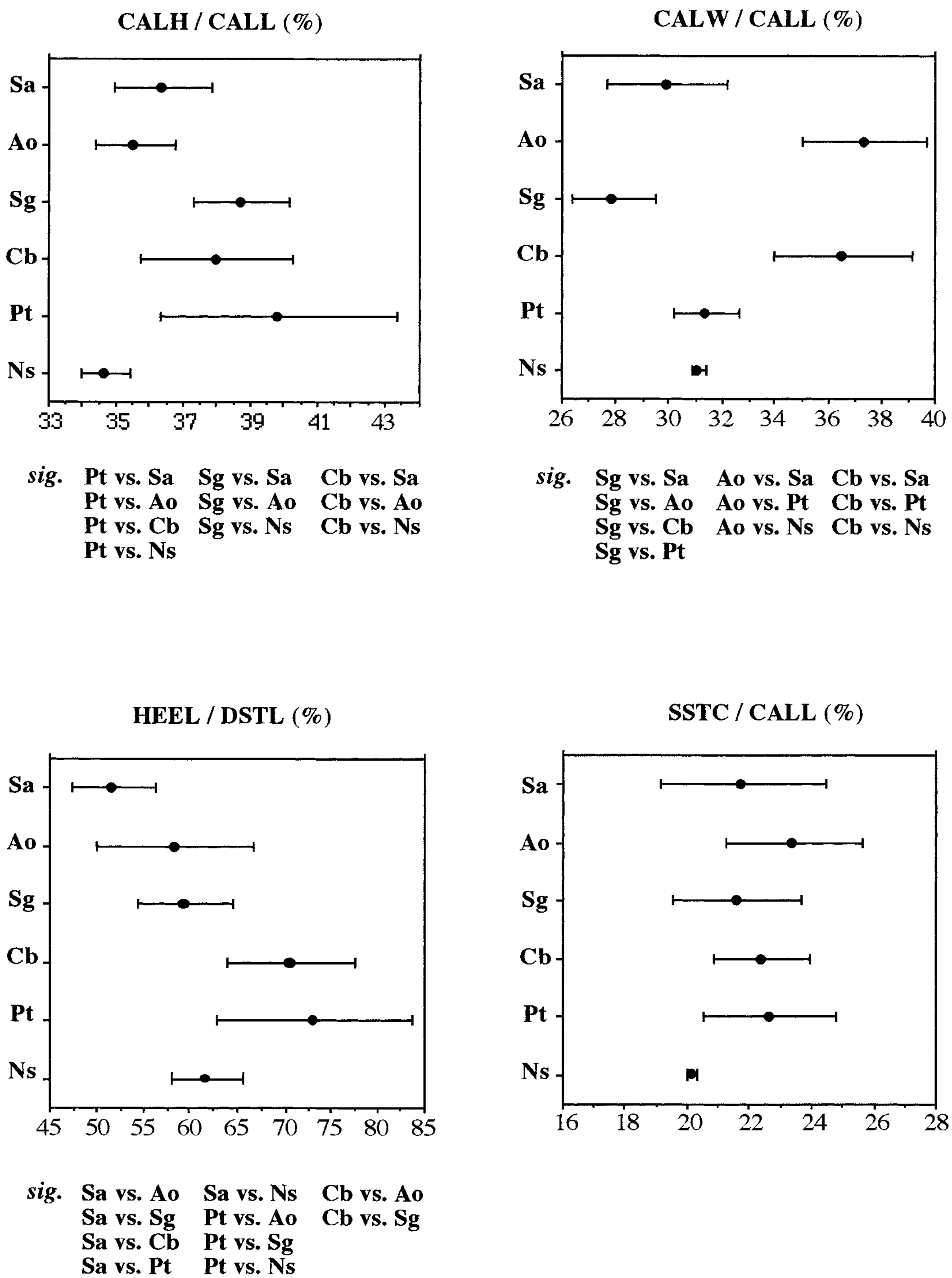

Fig. 15. Mean and ±1 standard deviation of calcaneal variables. Statistical difference was tested for by multiple comparison (Fisher's PLSD) at $P = 0.05$ and significantly different pairs are shown below each plot. For species name, see Figure 4.

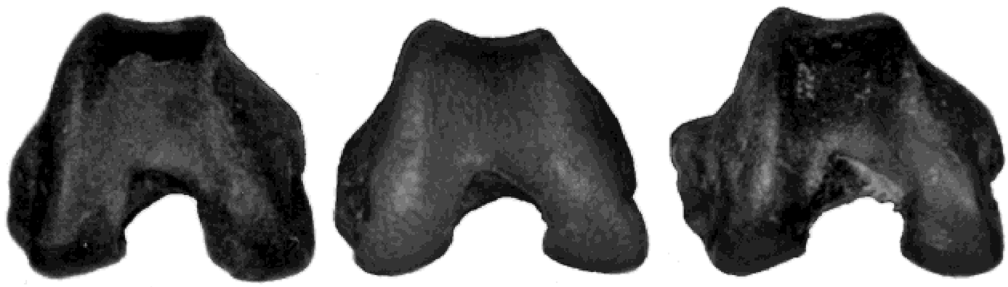

Fig. 16. Distal view of the right femur of extant *Saimiri* specimens housed in the American Museum of Natural History (left: 188110, center: 211613, right: 211600).

Affinity to extant platyrrhines

The size category of the fossil specimens is close to that of *Saimiri*. The femoral head (n = 5) and talus (n = 4) allow a good estimation of the average of and the variation in skeletal size in *Neosaimiri*. Averages are slightly smaller than those of *Saimiri* (Tables 5, 8), but they are not statistically different.

The postcranium of *Neosaimiri* exhibits the following features (Table 10). The articular surface of the humeral head is superoinferiorly long and demarcated by a distinct grove laterally. The humeral tuberosities are moderately large and the bicipital groove is shallow. The proximal humerus is most similar to that of *Saimiri* and *Saguinus* although these taxa lack a groove along the lateral border of the humeral head.

The proximal ulna of *Neosaimiri* characteristically exhibits a long olecranon. Its medial surface is excavated at the origin of *m. flexor digitorum profundus*. The coronoid process is moderately high. The morphology of the proximal ulna, particularly the length of the olecranon, most resembles the condition in *Saguinus* if the absolute size is not considered.

The proximal femur of *Neosaimiri* exhibits a shallow articular surface and a very thick neck with a well-developed tubercle for the ischiofemoral ligament. These features are most similar to those of *Saguinus*. The distal region of the femur is not well preserved. However, the following features are revealed. The femoral condyles are anteroposteriorly moderately deep and less asymmetrical in width, resembling the condition in *Aotus*. The patellar surface of *Neosaimiri* (based on IGM-KU 89187 and 89189) is narrow and moderately excavated with symmetrically raised patellar lips, being similar to the condition in *Saimiri, Aotus,* and *Saguinus*.

The distal region of the tibia is moderately wide. The surface marks on the lateral side suggest the development of the tibiofibular syndesmosis. The anterior beak of the distal surface is small and the anterior extension of the distal articular surface is not well developed. This condition is more or less alike that of *Saimiri, Aotus,* and *Saguinus*. However, none of these living taxa is exactly the same. *Aotus* differs from *Neosaimiri* in the relatively poor development of the ligamnentous insertions for the tibiofibular syndesmosis, and both *Saimiri* and *Saguinus* exhibit a more developed anterior beak and anterior extension of the distal articular surface.

The talar trochlea of *Neosaimiri* is narrow and quadrilateral on the dorsal aspect and lacks a depression at the middle of the distal region. The tibial malleolar facet is small. The neck is moderately long and the head is small and modestly flattened. This configuration does not match the character states in the living taxa. However, *Saimiri* shows a relatively close affinity. They differ only in the presence of the depression at the distal region of the midtrochlea and the less flattened talar head in *Saimiri*. The rest living taxa differ from *Neosaimiri* in the overall proportions, such as trochlear width or head size.

The calcaneus of *Neosaimiri* is slender and dorsoplantarly low (or proximodistaly

TABLE 10. Postcranial characters of Neosaimiri *and extant platyrrhines*

Neosaimiri	*Saimiri*	*Aotus*	*Saguinus*	*Cebus*	*Pithecia*
Proximal humerus					
humeral head *long*	long	wide	long	long	wide
greater tuberosity diameter *moderately large*	moderately large	moderately large	moderately large	very large	moderately large
lesser tuberosity diameter *large*	large	small	large	small	large
groove *present* along the lateral border of the superior articular surface	absent	present	absent	present	present
bicipital groove *shallow*	shallow	shallow	shallow	deep	shallow
Proximal ulna					
olecranon *very long*	moderately long	moderately long	very long	moderately long	short
coronoid process *moderately high*	moderately high	moderately or very high	moderately high	very high	moderately high
m. flexor digitorum profundus origin excavated *deeply*	shallow	deep	deep	deep	shallow
Femur					
articular surface of the head *shallow*	shallow	shallow	shallow	shallow	deeper
neck *very robust*	robust	robust	very robust	less robust	robust
tubercle behind the neck *developed*	small	small	developed	absent	small
distal epiphysis *moderately deep*	very/moderately deep	moderately deep	moderately deep	shallow	very shallow
medial condyle *not enlarged* relative to the lateral condyle	enlarged	not enlarged	enlarged	enlarged	enlarged
patellar surface *deep* (89187, 89189) *very deep* (89188)	deep	deep	deep	very deep	shallow
patellar surface lips *symmetrical* (89187, 89189) *lateral lip elevated* (89188)	symmetrical	symmetrical	symmetrical	lateral lip elevated	lateral lip elevated
patellar surface *narrow*	narrow	narrow	narrow	wide	very wide
distal tibia					
epiphysis *moderately wide*	moderately wide	moderately wide	moderately wide	very wide	very wide
tibiofibular syndesmosis *developed*	developed	weak	developed	weak	remarkably developed
anterior beak of the distal surface *small*	large	small	large	large	medium
anterior extension of the articular surface *absent*	present	variable	present	variable	present
Talus					
trochlea lips *parallel*	parallel	parallel	parallel	parallel	posteriorly wedged
trochlea *narrow*	narrow	very narrow	very wide	narrow	wide
depression at the middle of the distal trochlea *absent*	present	absent	weak	present	absent
tibial maelollar facet *small*	small	small	small	large	small
talar neck *moderately long*	moderately long	moderately long	long	moderately long	short
talar head *small*	small	large	small	moderately large	moderately large
talar head *moderately flattened*	not flattened	moderately flattened	moderately flattened	not flattened	flattened
Calcaneus					
body of calcaneus *low*	low	low	moderately high	moderately high	high
body of the calcaneus *slender*	slender	wide	slender	wide	slender
calcaneal tuberosity *moderately long*	short	moderately long	moderately long	long	long
medial facet *moderately small*	small	small	small	large	large
proximal facet *moderately long*	long	long	long	short	long

long). The calcaneal tuberosity is moderately elongated relative to the distal region. The proximal facet is long and moderately inclined, and the sustentaculum tali is short accompanying a small medial facet. Overall, this configuration is most similar to the *Saimiri* calcaneus although the calcaneal tuberosity is longer as compared with *Saimiri*. A similar degree of calcaneal tuberosity elongation is found in *Aotus* and *Saguinus*. But, these taxa differ from *Neosaimiri* in the emphasized mediolateral and dorsoplantar dimension, respectively.

As a whole, the postcranial skeleton of *Neosaimiri* described here exhibits a remarkable affinity to extant *Saimiri* in size and shape among the medium-sized living platyrrhines although some traits show a resemblance to *Saguinus* (long olecranon, stout femoral neck) or *Aotus* (moderately deep and less asymmetrical femoral condyles). This result is concordant with the previous analyses of postcrania (Gebo et al., 1990; Meldrum et al., 1990; Meldrum and Kay, 1997) and also supports the phylogenetic affinity between *Neosaimiri* and *Saimiri* advocated by the dental remains (e.g., Takai, 1994). On the other hand, the differences between these two taxa, recognized in several traits, are very important for inferring the locomotor evolution of *Saimiri*. At the same time, these differences support a generic distinction between *Neosaimiri* and *Saimiri* (Takai, 1994; contra Rosenberger et al., 1991b). Implications for the general locomotor profile in *Neosaimiri* and the locomotor and morphological differences between these taxa are discussed in the following sections.

Function and locomotor behavior

The humeral head of *Neosaimiri*, which is superoinferiorly long and elevated above the humeral tuberosities, perhaps allows a good deal of flexion at the glenohumeral joint (Schön Ybarra and Schön, 1987). The humeral tuberosities are located along the sides of the articular surface, providing the rotator cuff muscles widespread areas of insertion (Fleagle and Simons, 1982). The modestly wide superior surface and narrow posterior surface of the humeral head is an obvious adaption for flexion and extension, a basic functional requirement for quadrupedal progression. The bicipital groove of *Neosaimiri* is wide and shallow as in quadrupedal-leaping platyrrhines and unlike that of suspensory primates where the bicipital groove is narrow and deep (Rose, 1989). Muscular marks on the proximal humerus of *Neosaimiri* are rugose, suggesting well-developed rotator cuff muscles, which produce powerful flexion of the arm and/or fixation of the joint (e.g., Larson and Stern, 1989). The groove on the lateral border of the humeral head suggests a tough joint capsule. From this, it might be inferred that forelimbs functioned in important ways in locomotor or postural behaviors in *Neosaimiri*.

The olecranon of *Neosaimiri* is long and straight, providing a long moment arm for *m. triceps brachii* to extend the elbow from a fairly flexed position (Jolly, 1967; Conroy, 1974; Rose, 1993). In addition, a straight olecranon, rather than posteriorly flexed, is not adaptive for full extension of the elbow (Jolly, 1967; Birchette, 1982). Thus, *Neosaimiri* could gain a good deal of muscular force at the elbow with the forearm deeply or partially flexed, which may be required during the support phase of arboreal quadrupedalism (Walker, 1974; Rose, 1993). *Neosaimiri* has a moderately high coronoid process like other similar-sized extant platyrrhines. It has been claimed that a relatively low coronoid process is a feature of arboreal primates because its low height is primarily related to a relatively lower degree of elbow extension (Conroy, 1974). This feature also confirms a less-extended elbow joint position in *Neosaimiri*. Like the proximal humerus, the proximal ulna of *Neosaimiri* exhibits well-developed attachments for such muscles as *triceps brachii*, *brachialis*, and *flexor digitorum profundus*.

The femoral head of *Neosaimiri* has a shallow articular surface with a modest proximoposterior extension. The extent of the articular surface is closely related to the mode of locomotor and postural behaviors. A shallow articular surface permits a modest degree of flexion-extension of the thigh without great abduction, and is thus associated with cursorial locomotion (Jenkins and Camazine, 1977). On the other hand, a deeper surface with a posterosuperior exten-

sion reflects the extreme extension of the adducted hindlimb or lateral rotation of the thigh combined with adduction, and is often found in specialized leapers (Walker, 1974; Fleagle, 1976; Fleagle and Meldrum, 1988; Anemone, 1993), although the joint extension of the femoral head has not yet been explained thoroughly (e.g., Ford, 1988; Dagosto and Schmid, 1996). The morphology of the *Neosaimiri* hip region suggests less specialized use. *Neosaimiri* probably engaged in leaping as well as quadrupedal walking and running, but it was not a specialized leaper such as *Pithecia*. In *Neosaimiri*, the neck of the femur is robust and displays a large tubercle behind the neck, which accommodates an insertion for the ischiofemoral ligament. This ligament would check an extreme flexion and medial rotation (Ford, 1980). Although its size and shape cannot be certainly correlated with a particular locomotor pattern (Ford, 1980, 1988), its greater size as well as the robustness of the neck suggests a relatively active locomotor behavior. The distal femur of *Neosaimiri* is anteroposteriorly deep, with the epiphyseal region being adapted for powerful and rapid extension of the knee due to the long moment arm of *m. quadriceps femoris* (Tardieu, 1981; Anemone, 1990, 1993). The femoral condyles of *Neosaimiri* are symmetrical, suggesting evenly distributed weights on both sides of the knee joint (Ford, 1988; Fleagle and Meldrum, 1988; Preuschoft, 1970). Therefore, it can be presumed that *Neosaimiri* moved its hindlimbs in a parasagittal plane, with limited abduction. This type of hindlimb excursion is useful in quadrupedal running and leaping (Fleagle, 1976; Fleagle and Meldrum, 1988). The patellar surface is narrow and moderately deep, suggesting patellar movements with restricted mediolateral slides, as opposed to the generalized arboreal quadrupeds (Rose, 1983). Flexion-extension of the knee is unlikely to involve a great deal of knee rotation (Hildebrand, 1988; Anemone, 1993; Gebo and Sargis, 1994).

The moderately wide distal tibia of *Neosaimiri* suggests less emphasized mediolateral movement. The talocrural joint of *Neosaimiri* promotes joint stability during dorsoplantarflexion, while restricting the abduction-adduction. This functional morphology is common among quadrupedal-leaping platyrrhines. The distal tibia of *Neosaimiri* bears the roughened surfaces, where the inferior tibiofibular ligaments are attached, suggesting a tight inferior tibiofibular syndesmosis. A tight tibiofibular syndesmosis restricts the talocrural joint to a hinge-like movement, allowing only dorsiflexion and plantarflexion (Dagosto, 1985; Lewis, 1989), and increases joint rigidity against external forces. Indeed, frequent leaping primates like *Saimiri* and *Pithecia* exhibit a similar condition (Table 10). Thus, this morphology suggests a relatively high frequency of leaping in *Neosaimiri*. Both IGM-KU tibiae have a smooth semilunar notch for the fibula, while IGM 250436 has a similar-shaped but rugose fibular notch (Meldrum and Kay, 1997). However, it is unlikely that this surface allows significant movements at the inferior tibiofibular articulation, by virtue of its small size and the well-developed marks for the inferior tibiofibular ligaments. In addition, the morphology of the fibular notch is rather variable among extant *Saimiri* specimens. No great functional difference can be presumed among these specimens.

In the *Neosaimiri* tibia, the anterior beak of the distal surface is relatively small, while some platyrrhines (*Saimiri* and *Saguinus*) exhibit a greater development of this feature. A large beak locks the lateral side of the talar neck when the talocrural joint is fully dorsiflexed. The small beak in *Neosaimiri* suggests a lower frequency of dorsiflexion or a lower degree of stresses. An extension of the distal articular surface on the anterior surface of the shaft is also related to this "locking" mechanism. This facet meets a trochlear surface extension on the talar neck during full dorsiflexion (Dagosto, 1986; Gebo, 1986; Meldrum, 1993). In *Neosaimiri*, the talocrural joint is not specialized for stability in the dorsiflexed position as much as it is in *Saimiri*, *Aotus*, and *Pithecia*. Although the behavioral feature related to such a function is hard to determine, it is suggested that a reliance on rapid running or long leaping may be comparatively less in *Neosaimiri*.

The quadrilateral talar trochlea of *Neosaimiri* probably provides a hinge-like ac-

tion that restricts abduction and adduction at the ankle joint. The less mobile inferior tibiofibular joint in *Neosaimiri* is concordant with the lack of posterior wedging of the trochlea. The proximally wedged trochlea with a medially inclined medial lip as seen in *Pithecia,* causes a lateral shift of the talar head with dorsiflexion, resulting in foot abduction (e.g., Dagosto, 1986; Strasser, 1988). This functional specialization is not developed in *Neosaimiri.* The talar trochlea of *Neosaimiri* lacks an obvious depression at the distal midregion (see Gebo et al., 1990; Meldrum, 1993). This depression is reciprocal to the large anterior tibial beak (Table 10). The absence of the depression in *Neosaimiri* suggests a somewhat less stable talocrural joint in the fully dorsiflexed position. The tibial malleolar facet of *Neosaimiri* is not particularly emphasized in size or concavity. It has been claimed that a large and deep malleolar facet is a feature associated with a frequent or specialized climbing, in which frequent dorsiflexion of the talocrural joint is required (e.g., Dagosto, 1986, 1988). The absence of these features suggests that *Neosaimiri* was not a specialized climber. The talar neck is moderately long in *Neosaimiri* as compared with extant platyrrhines. Although the length of the neck is linked to the magnitude of stresses and excursion at the midtarsal joint in supination and pronation (e.g., Langdon, 1984; Dagosto, 1988), the variation of the neck length in the examined taxa is complax and can not be clearly explained from behavioral features (Fig. 13, Table 8). However, the moderately long neck in *Neosaimiri* tali may be adapted for versatile functions and not for highly specialized positional activities. The talar head of *Neosaimiri* is small relative to the trochlea size and moderately flattened. The small talar head suggests the limited mediolateral movements as well as a relatively lower stress level. The flattened talar head prohibits the helical movements of the joint (Gebo and Sargis, 1994). The mobility of the transverse tarsal joint in *Neosaimiri* seems relatively but not markedly restricted.

The calcaneus of *Neosaimiri* is low and narrow. It exhibits a short sustentaculum tali. This morphology is similar to that of *Saimiri* and to a lesser extent *Aotus* and *Saguinus,* suggesting a narrow and less mobile foot, designed for cursorial locomotion. The *Neosaimiri* calcaneus has a relatively long calcaneal tuberosity with respect to the distal segment. The calcaneal tuberosity length estimates the power (in-lever) arm for *m. triceps surae* to plantarflex the foot and the length of the distal calcaneus is a part of the load (out-lever) arm (e.g., Hall-Craggs, 1965; Walker, 1967; Langdon, 1984; Ford, 1988). Thus, a longer power arm implies a larger plantarflexing force, while a longer load arm produces a greater velocity for propulsion. It is argued that a moderately long distal calcaneus is associated with quadrupedalism and a longer distal calcaneus with leaping, while primates specialized for climbing have a shorter distal length of the calcaneus (Gebo, 1989). The intrinsic proportion of the calcaneus does not thoroughly explain the variation in the extant taxa (the frequently leaping *Pithecia* has a proportionally long calcaneal tuberosity). Probably, the length of the cuboid or metatarsal needs to be considered in this case (e.g., Fleagle and Meldrum, 1988). The calcaneal tuberosity of *Neosaimiri* is as long as in *Aotus* and *Saguinus.* This suggests the presence of leaping and rapid running in the locomotor repertoire.

The *Neosaimiri* calcaneus exhibits a moderately long and narrow proximal facet, a small distal facet, and a small medial facet on the short sustentaculum tali. This condition of the subtalar articulation lacks any specialized feature and suggests a less derived locomotor mode in *Neosaimiri,* in which the foot contacts the substrate within a modest range of inversion-eversion, or there is only a modest degree of movement of the talus and leg on the calcaneus during the stance phase.

It is apparent that the postcranial bones of *Neosaimiri* exhibit a consistent functional signal, namely adaptation for rapid limb excursion within the parasagittal plane. They lack specializations for scansorial movements, hyperextension of the hip and knee joints, and powerful grasping movements of the foot which emphasize inversion. *Neosaimiri* presumably engaged in above-branch quadrupedal running and

walking and in frequent leaping across short gaps like *Saimiri, Aotus,* and *Saguinus.* The locomotor behavior of *Neosaimiri* appears to be best matched with the similar-sized *Saimiri.* However, several different character states (Table 10) suggest functional differentiations, which might be related to the difference in locomotor mode.

Neosaimiri and *Saimiri*

Gebo et al. (1990) suggested that the locomotor mode of *Neosaimiri* is quadrupedal-leaping with an emphasis on leaping, noting the resemblance of IGM-KU 88003 with the talus of living *Saimiri.* Meldrum et al. (1990) argued that the elbow of *Neosaimiri* exhibits adaptations for arboreal quadrupedal running among small supports, based on the morphology of the distal humerus (IGM 183512): that is, the dorsally angled medial epicondyle, prominent medial lip of the trochlea, and less spherical capitulum. Recently, Meldrum and Kay (1997) argue for a *Saimiri*-like locomotor repertoire in *Neosaimiri,* with an emphasis on frequent leaping on the basis of the well developed tibiofibular syndesmosis in a distal tibia (IGM 250436). The results of the present analysis based on new postcranial specimens largely coincide with these studies.

However, a few morphological differences do exist, some of which were noted in previous studies, and these features are evident among extant quadrupedal-leaping platyrrhines and between *Saimiri* and *Neosaimiri.* For example, *Saimiri* has a proportionally longer distal calcaneus (or a shorter calcaneal tuberosity) than *Aotus, Saguinus,* and *Neosaimiri.* This difference could be very important functionally since the calcaneal proportions affect the out- to in-lever ratios and indeed it is associated with locomotor differences among extant genera. Thus, *Saimiri* is a more frequent leaper than *Saguinus* (Fleagle and Mittermeier, 1980) and probably *Aotus* (Wright, 1981). In addition, the calcanei of *Neosaimiri* and *Saimiri* are very similar to each other except the relative length of the calcaneal tuberosity. It is unlikely this regional morphological difference is related to other functions more than the lever ratio of the triceps surae. It can be presumed the frequency of leaping and/or and rapid running in *Neosaimiri* could be lower than is *Saimiri.*

Despite the poor preservation, the surface condition of the postcranial bones of *Neosaimiri* suggest greater muscularity and rigidity at the shoulder, elbow, and hip joints. The long olecranon also suggests differences in elbow extension and quadrupedal progression. Further, the tibia and talus lack the morphological complex to stabilize the upper ankle joint during full dorsiflexion. The combination of all of these features suggests a lower frequency of cursorial locomotion (rapid running and leaping) and in turn a higher frequency of slower quadrupedalism in *Neosaimiri* relative to *Saimiri.* In sum, arboreal quadrupedal walking and running with frequent leaping is the primitive locomotor mode in the clade of *Neosaimiri* and *Saimiri.* But, the frequency of rapid running and/or leaping was probably lower in *Neosaimiri* than in *Saimiri.*

Evolution of the La Venta primates

Many species of La Venta primates are known by craniodental remains, representing the early divergence of extant New World taxa: for example, *Saimiri-Neosaimiri,* pitheciine-*Cebupithecia,* extant *Aotus-A. dindensis* (=*Mohanamico*?), callitrichines-*Micodon* and *Lagonimico, Alouatta-Stirtonia.* Unfortunately, however, postcranial remains of only four taxa (including one uncertain taxon) have been discovered in La Venta.

Neosaimiri was originally discovered at the UC (University of California) locality V4517 at Los Mangos Area in the 1940s (Stirton, 1951). The horizon of this site is referred as to the “Monkey Unit” of Fields (1959; see Takai et al., 1992). The age of the “Monkey Unit” is estimated as about 16.1 million years old by the fission-track method (Takemura and Danhara, 1985). Postcranial remains were not discovered until the 1990s. At present, most of *Neosaimiri* specimens are found at the Masato Site in the El Cusco area. The age of this site is estimated at about 12.6–13.6 Ma by the fission-track method (Takemura et al., 1992) and 12.2 Ma by the $^{40}Ar/^{39}Ar$ method (Guerrero, 1997). One distal humerus (IGM 183512) was discovered at the Duke locality 54 in the Los Mangos area (Meldrum et al., 1990). This

locality corresponds to the same horizon as the "Monkey Unit" and is thus older than the Masato Site by 2.5–3.9 million years. Although no distal humerus has been collected from the Masato Site, there is no contradiction in the functional signal presented by the materials discovered from the both sites.

At the UC locality V4517, *Cebupithecia sarmientoi* was found together with *Neosaimiri* (Stirton, 1951). At present, *Cebupithecia* is the postcranially best known fossil platyrrhine from La Venta: the holotype (UCMP 38762) preserves about 70% of the postcranium. Its postcranium exhibits both similarities and dissimilarities with that of extant *Pithecia* (Fleagle and Meldrum, 1988; Meldrum and Fleagle, 1988; Ford, 1990). Recently, further postcranial fossils were discovered at the Duke Locality 21 of San Alfonso (Meldrum et al., 1990; Meldrum and Kay, 1997) and the Duke Locality 79 of Cerro Gordo (Meldrum and Kay, 1990), completing the holotype. The horizon of these sites is about 400 m lower that the Monkey Unit.

A talus of *Aotus dindensis* was discovered at the Kyoto Locality 9-86A of El Dinde (Gebo et al., 1990), the horizon of which corresponds to the lowest part of the Molina Member (Takai et al., 1992). This talus is very similar to that of extant *Aotus*, and an *Aotus*-like quadrupedal-leaping locomotion with a somewhat more emphasis on leaping is suggested (Gebo et al., 1990).

Although its taxonomic status is uncertain, one talus was discovered at the Duke locality 43 of El Cusco (Ford et al., 1991). The horizon of this site is close to that of the Masato site (Takai, 1995). This *Callicebus*-like-sized talus is different from those of *Cebupithecia* and *Neosaimiri* morphologically, and exhibits similarities to extant callitrichines and to a lesser extent to large atelines (Ford et al., 1991).

Among these four La Venta platyrrhines, only *Neosaimiri* and *Cebupithecia* are represented by a wealth of postcranial remains. As for *Cebupithecia,* Ford (1990) claimed a somewhat modern *Pithecia*-like locomotor repertoire, which includes quadrupedal branch running, leaping, some climbing, and suspensory behaviors. Meldrum (1993) argued that there was a similar differentiation of the forest utilization in *Neosaimiri* and *Cebupithecia* as that of *Saimiri* and *Pithecia*. Interestingly, *Cebupithecia* has adapted to the *Pithecia*-like locomotor pattern structurally in a different way (Ford, 1990). The postcranium of *Cebupithecia* is less derived relative to modern pitheciines in several features which are related to climbing and suspensory behaviors (Meldrum, 1993). Likewise, *Neosaimiri* is presumed to have depended on leaping and/or rapid running less frequently relative to extant *Saimiri*. It may be implied that such locomotor differences between Miocene and modern counterparts reflect a somewhat different forest structure or less developed niche separation in foraging and diet despite the fact that an analogous ecological diversity had appeared in Colombia by ca 15 Ma. However, this speculation must wait more comprehensive knowledge of locomotor profile and dietary habits of the La Venta primates.

Among extant platyrrhines, the phylogenetic position of *Saimiri* is controversial. While Rosenberger (1984) and Ford (1986) advocate a clade of *Saimiri* and *Cebus,* Kay (1990) claims a relationship to Callitrichinae. The former two authors further differ in the position of the *Saimiri-Cebus* clade: sister group of Callitrichinae constituting Cebidae (Rosenberger, 1984) and out group relative to all of the rest platyrrhines (Ford, 1986). Postcrania of *Neosaimiri* exhibit a resemblance to those of *Saguinus* regarding the morphology of the olecranon and femoral head. However, these coincidences do not necessarily imply the proximity to Callitricinae because the present study does not reveal the morphotype of Callitrichinae. At any rate, since *Neosaimiri* and *Saimiri* are very similar in the skeletal morphology, the postcranial morphology of *Neosaimiri* alone gives limited information to the phylogeny of the platyrrhines without the postcrania of *Micodon* or *Lagonimico* or the unknown ancestral stock of *Cebus.* Further discoveries of postcranial specimens will help to clarift the locomotor differentiation in the La Venta primates and the evolutionary history of extant platyrrhines.

ACKNOWLEDGMENTS

The authors thank all the staff of INGEOMINAS for collaboration in the field

work at La Venta. We thank Drs. S.M. Ford, D.L. Gebo, A.L. Rosenberger, E.J.E. Szathmary, and an anonymous associate editor for comments to improve the quality of earlier versions of manuscript, Prof. H. Ishida for thoughtful discussions to this study, and Prof. M.D. Rose for reading the draft of this paper. We are very grateful to Dr. D.J. Meldrum for sending us a reprint of his paper and casts of *Neosaimiri* fossils. Drs. B.D. Patterson of the Field Museum of Natural History, B. Mader of the American Museum of Natural History, and N. Shigehara of the Primates Research Institute of Kyoto University kindly arranged accesses to primates skeletal specimens under their care.

LITERATURE CITED

Anemone RL (1990) The VCL hypothesis revisited: patterns of femoral morphology among quadraupedal and saltatorial prosimian primates. Am. J. Phys. Anthropol. *83:*373–393.

Anemone RL (1993) The functional anatomy of the hip and thigh in primates. In DL Gebo (ed.): Postcranial Adaptation in Nonhuman Primates. Dekalb: Northern Illinois University Press, pp. 150–174.

Birchette MG (1982) The Postcranial Skeleton of *Paracolobus chemeroni.* Ph.D. dissertation, Harvard University.

Boinski S (1989) The positional behavior and substrate use of squirrel monkeys: Ecological implications. J. Hum. Evol. *18:*659–677.

Conroy G (1974) Primate Postcranial Remains from the Fayum Province, Egypt. Ph.D. dissertation, Yale University.

Dagosto M (1985) The distal tibia of primates with special reference to the Omomydae. Int. J. Primatol. *6:*45–75.

Dagosto M (1986) The Joints of the Tarsus in Strepsirhine Primates: Functional, Adaptive, and Evolutionary Implications. Ph.D. dissertation, City University of New York.

Dagosto M (1988) Implications of postcranial evidence for the origin of euprimates. J. Hum. Evol. *17:*35–56.

Dagosto M, and Schmid P (1996) Proximal femoral anatomy of omomyiform primates. J. Hum. Evol. *30:*29–56.

Fields RW (1959) Geology of the La Venta Badlands, Colombia, South America. Univ. Calif. Publs. Geol. Sci. *32:*405–444.

Fleagle JG (1976) Locomotor behavior and skeletal anatomy of sympatric Malaysian leaf-monkeys (*Presbytis obscura* and *Presbytis melalophos*). Yrbk. Phys. Anthropol. *20:*440–453.

Fleagle JG (1988) Primate Adaptation and Evolution. San Diego: Academic Press.

Fleagle JG, and Meldrum DJ (1988) Locomotor behavior and skeletal morphology of two sympatric pitheciine monkeys, *Pithecia pithecia* and *Chiropotes satanas.* Am. J. Primatol. *16:*227–249.

Fleagle JG, and Mittermeier RA (1980) Locomotor behavior, body size, and comparative ecology of seven Surinam monkeys. Am. J. Phys. Anthropol. *52:*301–314.

Fleagle JG, and Simons EL (1982) The humerus of *Aegyptopithecus zeuxis:* A primitive anthropoid. Am. J. Phys. Anthropol. *59:*175–193.

Ford SM (1980) A Systematic Revision of the Platyrrhini Based on Selected Features of Postcranium. Ph.D. dissertation, University of Pittsburgh.

Ford SM (1986) Systematics of the New World monkeys. In DR Swindler and J Erwin (eds.) Comparative Primate Biology, vol. 1: Systematics, Evolution and Anatomy. New York: Alan R. Liss, pp. 73–135.

Ford SM (1988) Postcranial adaptations of the earliest platyrrhine. J. Hum. Evol. *17:*155–192.

Ford SM (1990) Locomotor adaptations of fossil platyrrhines. J. Hum. Evol. *19:*141–173.

Ford SM, Davis LC, and Kay RF (1991) New Platyrrhine astragalus from the Miocene of Colombia. Am. J. Phys. Anthropol. Suppl. *12:*73–74.

Garber PA (1991) A comparative study of positional behavior in three species of tamarin monkeys. Primates *32:*219–230.

Gebo DL (1986) The Anatomy of Prosimian Foot and Its Application to the Primate Fossil Record. Ph.D. dissertation, Duke University.

Gebo DL (1989) Locomotor and phylogenetic considerations in anthropoid evolution. J. Hum. Evol. *18:*201–233.

Gebo DL (1993) Functional morphology of the foot in primates. In DL Gebo (ed.): Postcranial Adaptation in Nonhuman Primates. DeKalb: Northern Illinois University Press, pp. 175–196.

Gebo DL, Dagosto M, Rosenberger AL, and Setoguchi T (1990) New platyrrhine tali from La Venta, Columbia. J. Hum. Evol. *19:*737–746.

Gebo DL, and Sargis EJ (1994) Terrestrial adaptations in the postcranial skeletons of guenons. Am. J. Phys. Anthropol. *93:*341–371.

Guerrero J (1997) Stratigraphy and sedimentary environments of the Honda Group in the La Venta area, Miocene uprift of the Colombian Andes. In RF Kay, RH Madden, RL Ciffeli, and JJ Flynn (eds.): A History of Neotropical Fauns: Vertebrate Paleobiology of the Miocene of Tropical South America. Washington DC: Smithonian Institute Press, (in press).

Hall-Craggs ECB (1965) An osteometric study of the hind limb of the Galagidae. J. Anat. *99:*119–126.

Hildebrand M (1988) Analysis of Vertebrate Structure. New York: John Wiley and Sons, Inc.

Jenkins FA, and Camazine SM (1977) Hip structure and locomotion in ambulatory and cursorial carnivores. J. Zool. Lond. *181:*351–370.

Jolly CJ (1967) The evolution of baboons. In H Vagbourg (ed.): The Baboon in Medical Research, vol 2. Austin: University of Texas Press, pp. 23–50.

Kay RF (1990) The phyletic relationships of extant and fossile Pitheciinae (Platyrrine, Anthropoidea). J. Hum. Evol. *19:*175–208.

Langdon JH (1984) Functional Morphology of the Miocene Hominoid Foot. Basel: Karger.

Larson SG, and Stern JT (1989) Role of supraspinatus in the quadrupedal locomotion of vervets (*Cercopithecus aethiops*): Implication for interplitation of humeral morphology. Am. J. Phys. Anthropol. *79:*369–377.

Lewis OJ (1989) Functional Morphology of the Evolving Hand and Foot. Oxford: Clarendon Press.

Meldrum DJ (1993) Postcranial adaptations and positional behavior fossil platyrrhines. In DL Gebo (ed.): Postcranial Adaptation in Nonhuman Primates. DeKalb: Northern Illinois University Press, pp. 235–251.

Meldrum DJ, and Fleagle JG (1988) Morphological affinities of the postcranial skeleton of *Cebupithecia sarmientoi.* Am. J. Phys. Anthropol. *75:*249–250.

Meldrum DJ, Fleagle JG, and Kay RF (1990) Partial humeri of two Miocene Colombian primates. Am. J. Phys. Anthropol. *81:*413–422.

Meldrum DJ, and Kay RF (1990) A new partial skeleton of *Cebupithecia sarmientoi* from the Miocene of Colombia. Am. J. Phys. Anthropol. *81:*267.

Meldrum DJ, and Kay RF (1997) Postcranial skeletal morphology of the fossil platyrrhines from the Miocene of Colombia. In RF Kay, RH Madden, RL Ciffeli, and JJ Flynn (eds.): A History of Neotropical Fauns: Vertebrate Paleobiology of the Miocene of Tropical South America. Washington DC: Smithnian Institute Press, (in press).

Moyniham M (1976) The New World Primates. Princeton: Princeton University Press.

Preuschoft H (1970) Functional anatomy of the lower extremity. In GH Bourne (ed.): The Chimpanzee. Basel: Karger, pp. 221–294.

Rose MD (1983) Miocene hominoid postcranial morphology monkey-like, ape like, neither, or both? In RS Chiochon and RS Corruccini (eds.): New Interpretations of Ape and Human Ancestry. New York and London: Plenum Press, pp. 405–417.

Rose MD (1989) New postcranial specimens of catarrhines from Middle Miocene Chinji formation, Pakistan: Descriptions and a discussion of proximal humeral functional morphology in anthropoids. J. Hum. Evol. *18:*131–162.

Rose MD (1993) Functional anatomy of the elbow and forearm in primates. In DL Gebo (ed.): Postcranial Adaptation in Nonhuman Primates. DeKalb: Northern Illinois University Press, pp. 70–95.

Rosenberger AL (1984) Fossil New World monkeys dispute the molecular clock. J. Hum. Evol. *13:*737–742.

Rosenberger AL, Setoguchi T, and Shigehara N (1990) The fossil record of callitricine primates. J. Hum. Evol. *19:*209–236.

Rosenberger AL, Setoguchi T, and Hartwig WC (1991a) *Laventiana annectens,* new genus and species: Fossil evidence for the origins of callitrichine New World monkeys. Proc. Natl. Acad. Sci. USA *88:*2137–2140.

Rosenberger AL, Hartwig WC, Takai M, Setoguchi T, and Shigehara N (1991b) Dental variability in Saimiri and the taxonomic status of *Neosaimiri fieldsi,* an early squirrel monkey from La Venta, Colombia. Int. J. Primatol. *12:*291–301.

Schön-Ybarra MA, and Schön MA (1987) Positional behavior and limb bone adaptations in red howling Monkeys (*Alouatta seniculus*). Folia Primatol. *49:*70–89.

Stirton RA (1951) Ceboid Monkeys from the Miocene of Colombia. Univ. Calif. Publ. Geol. Sci. *28:*315–356.

Strasser E (1988) Pedal evidence for the origin and diversification of cercopithecid clades. J. Hum. Evol. *17:*225–245.

Szalay FS, and Delson E (1979) Evolutionary History of the Primates. New York: Academic Press.

Takai M (1994) New specimens of *Neosaimiri fieldsi* from La Venta, Colombia: A middle Miocene ancestor of the living squirrel monkeys. J. Hum. Evol. *27:*329–360.

Takai M (1995) Preliminary review of the specimens and localities of platyrrhine fossils from the Tatacoa Desert, Colombia. Kyoto Univ. Overseas Res. Report of New World monkeys *9:*1–22.

Takai M, Takemura K, Takemura A, Villarroel C, Hayashida A, Danhara T, Ohno T, Franco R, Setoguchi T, and Nogami Y (1992) Geology of La Venta, Colombia, South America. Kyoto Univ. Overseas Res. Reports of New World monkeys *5:*31–38.

Takemura K, and Danhara T (1985) Fission-track dating of the upper part of the Miocene Honda Group in La Venta Badlands, Colombia. Kyoto Univ. Overseas Res. Reports of New World monkeys *5:*31–38.

Takemura K, Takai M, Danhara T, and Setoguchi T (1992) Fission-track ages of the Villavieja Formation of the Miocene Honda Group in La Venta, Department of Hulia, Colombia. Kyoto Univ. Overseas Res. Reports of New World monkeys *8:*19–27.

Tardieu C (1981) Morpho-functional analysis of the articular surfaces of the knee-joint in primates. In AB Chiarelli and RS Corruccini (eds.): Primate Evolutionary Biology. Berlin: Springer-Verlag, pp. 68–80.

Terborgh J (1983) Five New World Primates. A Study in Comparative Ecology. Princeton: Princeton University Press.

Walker AC (1967) Locomotor Adaptations in Recent and Fossil Madagascan Lemur. Ph.D. thesis, University of London.

Walker A (1974) Locomotor adaptations in past and present prosimian primates. In FA Jenkins (ed.): Primate Locomotion. London: Academic Press, pp. 349–381.

Walker SE (1994) Positional behavior and habitat use in Chriopotes satanas and Pithecia pithecia. In B Thierry, JR Anderson, JJ Roeder, and N Herrenschmidt (eds.): Current Primatology. Strasbourg: Universite Louis Pasteur, pp. 195–201.

Wright PC (1981) The night monkeys, genus *Aotus.* In AF Coimbra-Filho and RA Mittermeier (eds.): Ecology and Behavior of Neotropical Primates. Rio de Janeiro: Academia Brasileira de Ciencias, pp. 211–240.